JACS
JOURNAL OF THE AMERICAN CHEMICAL SOCIETY
Article
pubs.acs.org/JACS

Kinetic and Thermodynamic Selectivity of Intermolecular C−H Activation at [Tp′Rh(PMe$_3$)]. How Does the Ancillary Ligand Affect the Metal−Carbon Bond Strength?

Yunzhe Jiao, James Morris, William W. Brennessel, and William D. Jones*

Department of Chemistry, University of Rochester, Rochester, New York 14627, United States

Supporting Information

ABSTRACT: Tp′Rh(PMe$_3$)(CH$_3$)H was synthesized as a precursor to produce the coordinatively unsaturated fragment [Tp′Rh(PMe$_3$)], which reacts with benzene, mesitylene, 3,3-dimethyl-1-butene, 2-methoxy-2-methylpropane, 2-butyne, acetone, pentane, cyclopentane, trifluoroethane, fluoromethane, dimethyl ether, and difluoromethane at ambient temperature to give only one product in almost quantitative yield in each case. All of the complexes Tp′Rh(PMe$_3$)(R)H were characterized by NMR spectroscopy, and their halogenated derivatives were fully characterized by NMR spectroscopy, elemental analysis, and X-ray crystallography. The active species [Tp′Rh(PMe$_3$)] was also able to activate the alkynyl C−H bond of terminal alkynes to give activation products of the type Tp′Rh(PMe$_3$)(C≡CR)H (R = *t*-Bu, SiMe$_3$, hexyl, CF$_3$, Ph, *p*-MeOC$_6$H$_4$, and *p*-CF$_3$C$_6$H$_4$). The measured relative rhodium−carbon bond strengths display two linear correlations with the corresponding carbon−hydrogen bond strengths, giving a slope of 1.54 for α-unsubstituted hydrocarbons and a slope of 1.71 for substrates with α-substitution. Similar trends of energy correlations were established by DFT calculated metal−carbon bond strengths for the same groups of substrates.

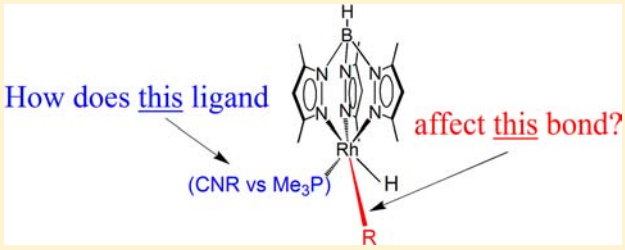

INTRODUCTION

The activation of C−H bonds by transition metal-based systems has a long history in modern chemistry. One of the most remarkable early discoveries was Shilov's system for converting methane to methanol catalyzed by Pt(II) in 1972.[1] The activation and functionalization of C−H bonds by homogeneous transition metal systems still remains attractive as innovative and economic catalyst systems are needed to meet the criteria of green chemistry.[2] Oxidative addition of C−H bonds is one of the most common routes to produce hydridohydrocarbyl metal complexes, which have been shown to undergo further functionalization such as carbonylation,[3−5] insertion of isocyanides[6−12] and unsaturated C−C bonds,[13−15] alkane dehydrogenation,[16−19] and borylation.[20−22] As the work of C−H functionalization progresses, understanding the factors that determine the high selectivity is critical to the advance of this field.

The process of oxidative addition is usually driven by photochemical or thermal generation of a transient coordinatively unsaturated intermediate that could form a three center σ-complex interaction with the substrate C−H bond and thereby facilitate insertion into the bond (eq 1).[23] Because the product stability is closely related to thermodynamic selectivity among different C−H bonds, a knowledge of relative M−C bond strengths is helpful to understand the factors controlling the product distribution. Methods to measure relative bond dissociation energy have been well studied and widely applied in C−H activation.[24−29] Typically, the relative thermodynamic stability (ΔG°) of the activation products can be derived from the equilibrium constant (K) (eq 2). Assuming that the entropy change is close to zero,[30] ΔH° is equal to ΔG°. The relative M−C bond strength is obtained from the known C−H bond strengths (eqs 3 and 4).

$$\Delta H = D_{\mathrm{R-H}} + D_{\mathrm{M-R'}} - (D_{\mathrm{R'-H}} + D_{\mathrm{M-R}}) \quad (3)$$

$$D_{\mathrm{rel}} = D_{\mathrm{M-R'}} - D_{\mathrm{M-R}} = -RT\ln(K) - D_{\mathrm{R-H}} + D_{\mathrm{R'-H}} \quad (4)$$

In previous examples, a linear correlation between M−C and C−H bond energies (defined as the slope $R_{\mathrm{M-C/C-H}}$) was well established, and the slopes are close to 1.1 in Wolczanski's (*t*Bu$_3$SiO)$_2$(*t*Bu$_3$SiNH)Ti(R) system (R contains 15 various alkyl, aryl, benzyl, and vinyl groups),[27] and a slope of 1.0 was found in his study of (*t*Bu$_3$NH)$_2$(*t*Bu$_3$-SiN═)Ta(R) (*R* = Ph, Me, benzyl).[28] Bercaw observed a trend with $R_{\mathrm{M-C/C-H}}$ = 1.29 in studies of Cp*$_2$Sc-R bond strengths (*R* = alkyl, phenyl, alkynyl).[29]

Received: August 5, 2013
Published: October 15, 2013

   dx.doi.org/10.1021/ja4080985 | J. Am. Chem. Soc. 2013, 135, 16198−16212

$$\Delta G^{\circ} = \Delta G^{\ddagger}_{re'} + \Delta\Delta G^{\ddagger}_{oa} - \Delta G^{\ddagger}_{re} \quad (5)$$

Our group has also examined the relationship between C−H bond energies and the corresponding Rh−C bond energies in complexes Tp′Rh(CNneopentyl)(R)H (R = alkyl, alkenyl, aryl). The thermodynamics for C−H bond activation were determined by combining reductive elimination with kinetic selectivity experiments as shown in Figure 1. Equation 5 was

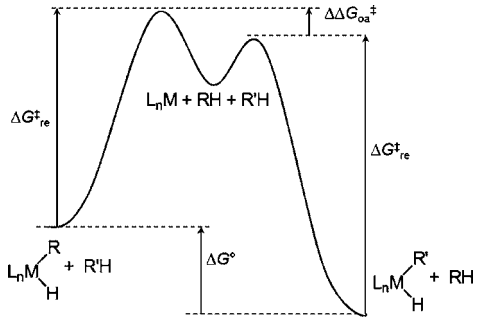

Figure 1. Free energy diagram for competitive C−H activation.

used to calculate the relative free energy, ΔG°, which was then used to determine relative Rh−C bond strengths for various hydrocarbon C−H bonds. With this kinetic technique, the relationship between sp^3 and sp^2 Rh−C and C−H bond strengths was found to be linearly correlated, although some curvature was noted in early studies.[31,32] The addition of data for alkyne sp C−H activation showed that all of these α-unsubstituted hydrocarbons followed a linear trend ($R_{M-C/C-H}$ = 1.38).[33] Subsequent work revealed that activation of substituted methyl derivatives (CH_3X or CH_2X_2) followed a different, but parallel trend ($R_{M-C/C-H}$ = 1.40), giving rise to products of the type Tp′Rh(CNneopentyl)(CH_2X)H (CH_2X = $CH_2CMe{=}CH_2$, α-mesityl, $CH_2C(O)CH_3$, $CH_2C{\equiv}CCH_3$, CH_2O-t-Bu, CH_2OMe, CH_2Cl, CH_2CN, CH_2F, CHF_2).[34,35] Both correlations showed almost identical slopes with the line for the α-substituted methyl derivatives lying ∼8 kcal mol^{-1} above the line (at D_{C-H} = 100 kcal mol^{-1}) for the unsubstituted hydrocarbons (Figure 2). This offset represents the additional M−C bond strength that is added based upon the strength of the C−H bond that is being broken; that is, the predicted M−C bond strength based on the strength of the C−H bond being broken is high by ∼8 kcal mol^{-1}. This increase was attributed to polarization of the bond (more ionic character) and hyperconjugation.[34,35]

In another study, the [Tp′Rh(CNneopentyl)] fragment was used to activate a variety of fluorinated benzenes. Once again, a correlation between Rh−aryl^F bond strengths and H−aryl^F bond strength was found, but now the slope was found to be 2.14, and the major factor affecting the Rh−aryl^F bond was the number of ortho fluorine substituents.[36] This same type of thermodynamic analysis was applied to a new metal fragment in which the π-acceptor neopentylisocyanide ligand was replaced by a σ-donating phosphine. The [Tp′Rh(PR_3)] fragments (R = PMe_3, PMe_2Ph) were tested in the correlation of Rh−C bond strength of fluoroaromatics.[37] Here, for R = PMe_2Ph, it was found that the slope of the correlation was 2.15, virtually identical to that seen with L = CNneopentyl. Perutz and Eisenstein investigated the effect of CO versus PH_3 spectator ligands in fluoroarene activation in [CpRe(CO)L], [CpRhL], and [CpIrL] complexes using DFT calculations. They found

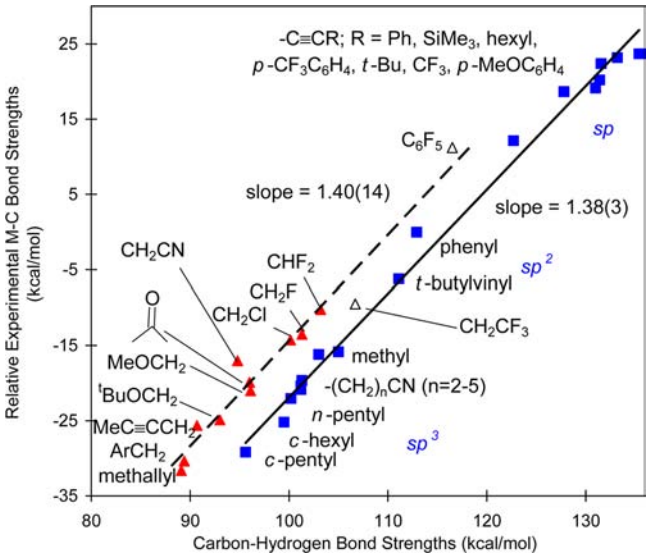

Figure 2. Plot of relative experimental M−C bond strengths vs C−H bond strengths. The solid line is fit to the hydrocarbons and aliphatic nitriles $-(CH_2)_n-CN$ (n = 2−5) (■, $y = 1.376x - 159.5$), and the dashed line is fit to the $-CH_2X$ substrates and $-CHF_2$ (▲, $y = 1.4024x - 154.6$). Also shown are $-C_6F_5$ and $-CH_2CF_3$ (Δ), which are not included in either fit. Experimental C−H bond strengths were used for all substrates except the alkynes and nitriles (except acetonitrile). Alkyne and nitrile C−H bond strengths were calculated (B3LYP) since experimental values are unavailable or have large errors. The vertical separation of the lines at D_{C-H} = 100 kcal mol^{-1} is 7.5 kcal mol^{-1}. Reproduced with permission from ref 35. Copyright 2013 American Chemical Society.

that the slopes $R_{M-C/C-H}$ varied by 0.18 for Re (2.25 vs 2.43), 0.45 for Rh (1.98 vs 2.43), and 0.46 for Ir (1.93 vs 2.39).[38]

Here, we investigate the effect of the spectator ligand in [Tp′RhL] for the activation of hydrocarbons, specifically for L = PMe_3, as was done with CNneopentyl. We examined both the parent hydrocarbons (sp, sp^2, and sp^3) and the α-substituted methyl derivatives ($-CH_2X$). While the stabilities of the C−H activation products are similar, the $R_{M-C/C-H}$ values for these derivatives are noticeably different, allowing a quantification of the effect of replacing a π-acceptor isonitrile spectator ligand with a σ-donor phosphine spectator ligand that is never trans to R or H.

■ RESULTS AND DISCUSSION

Synthesis and Characterization of Tp′Rh(PMe_3)(R)H. Irradiation of Tp′Rh(PMe_3)H_2 (**1**) has proven to be an efficient way to generate the reactive [Tp′Rh(PMe_3)] fragment, although formation of Tp′Rh(PMe_3)$_2$ can be problematic.[37] Photolysis of **1** in various hydrocarbons led to formation of Tp′Rh(PMe_3)(R)H (R = α-mesityl, ^{t}butylvinyl, CH_2O^tBu, $CH_2C{\equiv}CCH_3$, $CH_2C(=O)CH_3$, pentyl, cyclopentyl), as well as the side products (κ^2-Tp′)Rh(PMe_3)$_2$ and Tp′Rh(PMe_3)R_2. The yield was not improved at a lower temperature or in a quartz irradiation vessel. These byproducts presumably arise from photochemical decomposition of **1** or the target product Tp′Rh(PMe_3)(R)H.[39] As a consequence, Tp′Rh(PMe_3)(CH_3)H (**2**) was selected as a precursor to readily produce the [Tp′Rh(PMe_3)] fragment under ambient conditions ($t_{1/2}$ = 34.5 min for methane loss in benzene at 30.0 °C).

Treatment of Tp′Rh(PMe_3)Cl_2 with methylmagnesium chloride resulted in clean formation of Tp′Rh(PMe_3)(CH_3)Cl

dx.doi.org/10.1021/ja4080985 | J. Am. Chem. Soc. 2013, 135, 16198−16212

(**2**-Cl), which reacted with Cp_2ZrH_2 to give the hydride analog **2** (eq 6). The X-ray crystal structure of **2**-Cl shows an

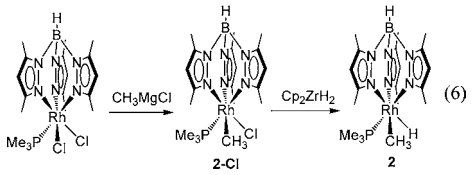

(6)

octahedral geometry with a Rh1−C16 distance of 2.062(6) Å, typical for a Rh−C (sp^3) bond. Isolation of zirconium-free **2** was problematic at first, because the $Rh(CH_3)H$ is so labile that it can easily exchange with the solvent to some extent during the synthesis and workup. For example, most of **2** is converted to $Tp'Rh(PMe_3)(C_6D_5)D$ after work up with benzene-d_6 as the solvent.[40] THF was finally chosen as a compromising solvent for the *in situ* reaction: first **2**-Cl is very soluble in THF compared with alkanes; second, only a small amount of $Tp'Rh(PMe_3)$(furanyl)H was observed, and the following exchange with the substrate will convert both **2** and $Tp'Rh(PMe_3)$(furanyl)H into the target product (Scheme 1).

Scheme 1. Products from Exchange of 2 in Various Substrates

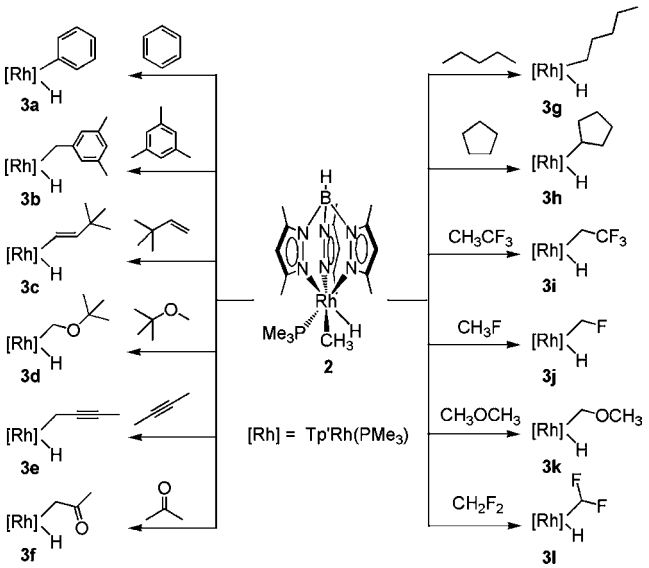

The reactions to form **3a**−**3h** were done in neat substrate. Reactions with gaseous substrates used a cyclohexane solution of **2** and 50 psi of substrate. Because these products were mostly air sensitive and hard to crystallize, only ^1H and $^{31}P\{^1H\}$ NMR spectroscopy was used for characterization. The more stable halogenated derivatives (**4b**−**g**, **4i**) were fully characterized by ^1H, $^{13}C\{^1H\}$, and $^{31}P\{^1H\}$ NMR spectroscopy, elemental analysis, and X-ray crystallographic analysis (eq 7).

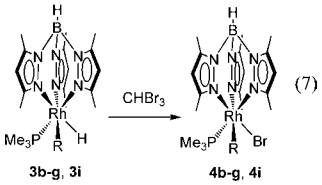

(7)

Compounds **4g**-Cl and **4h**-Cl were independently synthesized from the reaction of $Tp'Rh(PMe_3)Cl_2$ and related Grignard reagents. The formation of **3g** from reduction of **4g**-Cl also provides strong evidence for the suggested structure of **3g**. For **3h**, addition of bromoform or chloroform produced predominantly $Tp'Rh(PMe_3)X_2$ (X = Br or Cl). A broad doublet resonance was observed in the $^{31}P\{^1H\}$ NMR spectrum of **4h**-Cl suggesting hindered rotation of the cyclopentyl ring. The resonance appears as a sharp doublet at low temperatures (see Supporting Information). Addition of $AgBF_4$ to **4h**-Cl in THF-d_8 affords complete conversion of **4h**-Cl to a species assigned as $[Tp'Rh(PMe_3)(THF\text{-}d_8)H]^+BF_4^-$ (**6**), which is presumed to arise from β-elimination from intermediate $[Tp'Rh(PMe_3)(c\text{-pentyl})(THF\text{-}d_8)]^+BF_4^-$.

Synthesis of **3a** has been reported from photolysis of **1** in benzene,[41] but here we provide a new route to give clean formation of **3a** from thermal exchange of **2** in benzene. The ^1H NMR resonances of complex **2** and **3b**−**h** contain similar patterns for the hydride and Tp′ signals. In all cases, the hydride resonance was observed as a doublet of doublets between δ −17.1 and −18.7; the six resonances (3:3:3:3:3:3) between δ 2.1 and 2.8, as well as the three resonances (1:1:1) between δ 5.5 and 5.9, indicate the chirality at rhodium, and the κ^3-denticity of the Tp′ ligand is suggested from the crystal structures of their halogenated analogs.

It should be noted that all of the exchange reactions are almost quantitative and only give one major product with occasional traces of **1** or $Tp'Rh(PMe_3)(Cl)H$ (**5**) that remain from the preparation of **2**. No activation of the weaker secondary bonds was observed in the case of pentane. In the activation of 3,3-dimethyl-1-butene, only one vinyl C−H bond was cleaved (trans to ^{t}Bu) as seen with the CNneopentyl derivative.[32] Only methoxy C−H bonds were cleaved in the reaction of methyl *t*-butyl ether. In the activation of mesitylene, no observable formation of aryl hydride $Tp'Rh(PMe_3)(C_6H_2\text{-}2,4,6\text{-}Me_3)H$ was detected on the basis of the ^1H and $^{31}P\{^1H\}$ NMR resonances. This result differs from the photoreaction of Tp′Rh(CNneopentyl) in mesitylene, which produces a mixture of benzylic hydride and aryl hydride products in 3:1 ratio.[31] This may imply that $Tp'Rh(PMe_3)$ has greater kinetic selectivity than Tp′Rh(CNneopentyl), considering that the temperature used in this work and the previous photolysis of $Tp'Rh(CNneopentyl)(PhNCNCH_2CMe_3)$ are similar. More selectivity data are needed to support this hypothesis, however, as will be discussed.

Compounds **3a**, **3b**, and **3d** were synthesized by using RH as the solvent for the reaction of **2**-Cl and Cp_2ZrH_2 to first yield compound **2**, which then reacted with the solvent. However, for the other substrates, prior synthesis and isolation of **2** is necessary either because of the possible reaction between the zirconium species and the unsaturated solvent (in **3c**, **3e**, and **3f**) or the poor solubility of **2**-Cl and Cp_2ZrH_2 in pentane, cyclopentane, and gaseous substrates. Pressurization with CH_3CF_3 to *in situ* synthesized **2** in C_6D_{12} gave almost clean formation of $Tp'Rh(PMe_3)(CH_2CF_3)H$ (**3i**) after equilibrating for 1 day at ambient temperature. The hydride resonance of **3i** appears at δ −17.58 (dd, $^1J_{Rh-H}$ = 23.3 Hz, $^2J_{P-H}$ = 30.0 Hz). The splitting pattern and coupling constants are typical for this type $Tp'Rh(PMe_3)(R)H$, and it also indicates no additional coupling between the hydride and fluorine(s), which is further confirmed by ^{19}F NMR spectroscopy (Figure 3). $Tp'Rh(PMe_3)(CH_2F)H$ (**3j**) was prepared by reaction of **2** in C_6D_{12} with pressurized CH_3F at ambient temperature. **3j** contains a

dx.doi.org/10.1021/ja4080985 | J. Am. Chem. Soc. 2013, 135, 16198−16212

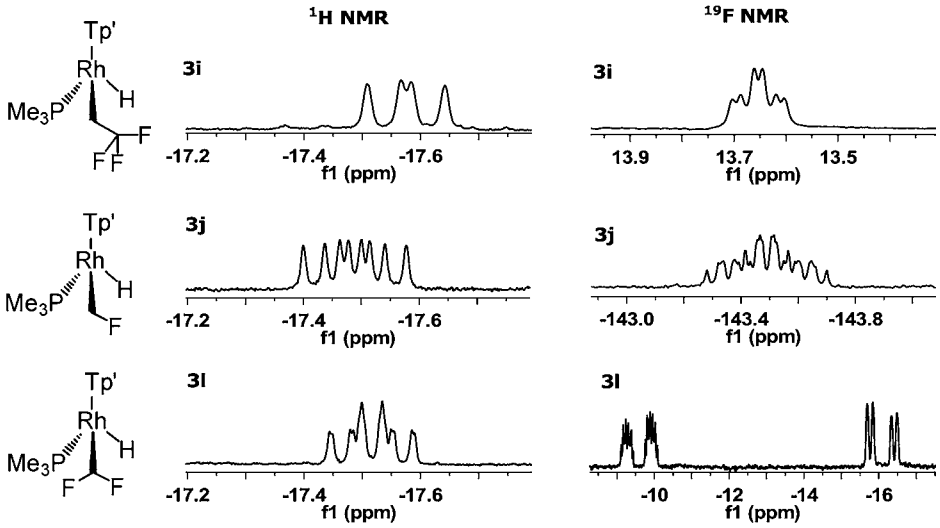

Figure 3. ^{1}H (only hydride resonances are shown) and ^{19}F spectra for complexes **3i**, **3j**, and **3l**. For **3i**, no direct coupling was observed of the hydride to the fluorine atom(s). For **3j**, direct coupling between the hydride and the fluorine atom is seen. For **3l**, only one of the two fluorine atoms couples to the hydride as indicated in the spectrum.

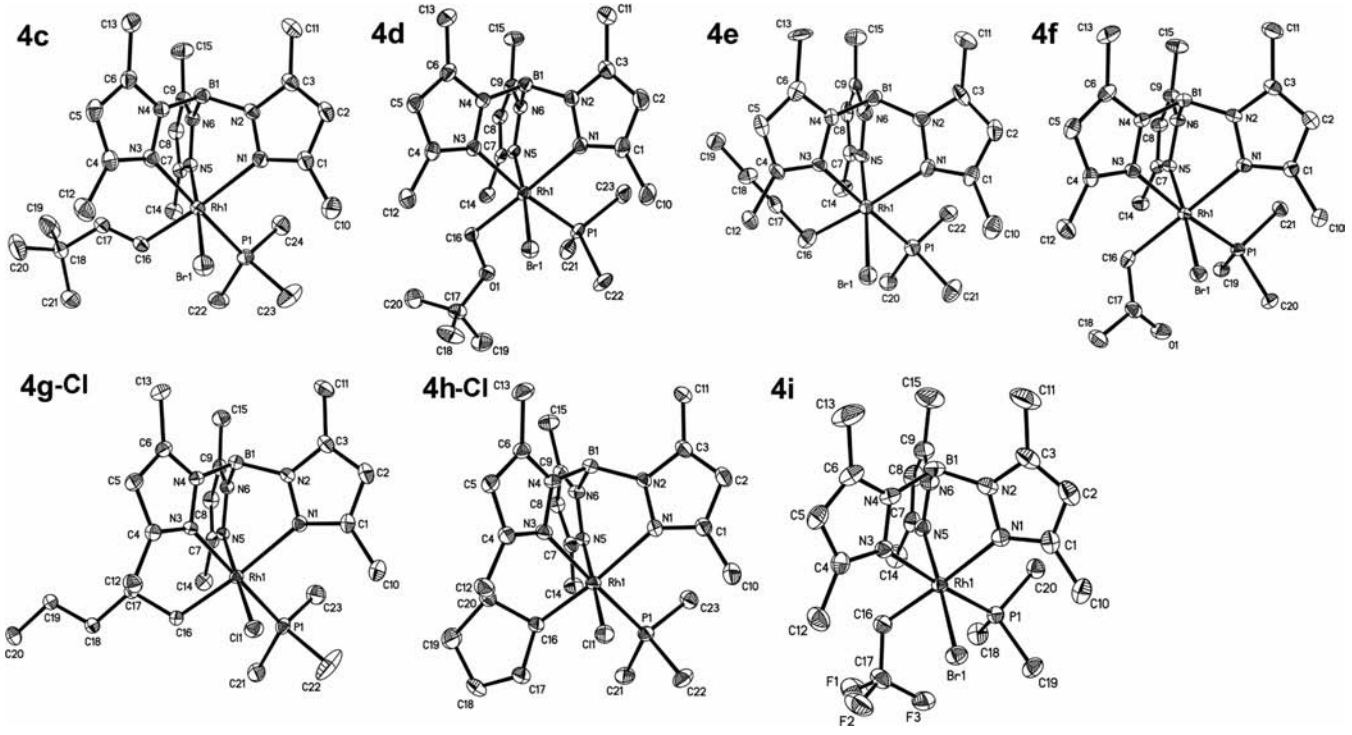

Figure 4. Thermal ellipsoid drawings of halogenated complexes **4c**−**4i** (thermal ellipsoids are shown at the 50% probability level). Hydrogen atoms were omitted for clarity.

fluoride-hydride coupling (J = 15 Hz) in it ^{1}H and ^{31}P NMR spectra. Because the purchased CH_3F contains ∼16% impurity of dimethyl ether, activation of both CH_3F and dimethyl ether was observed to give a 3.3:1 mixture of the corresponding activation products. As anticipated, the ^{1}H and ^{31}P NMR resonances of Tp′Rh(PMe$_3$)(CH$_2$OCH$_3$)H (**3k**) are quite similar to those of **3d**. A similar reaction of CH_2F_2 led to the exclusive C−H activation product Tp′Rh(PMe$_3$)(CHF$_2$)H (**3l**), which contains a hydride resonance coupled to the methylene hydrogen and one of the two fluorine atoms, as well as the rhodium and phosphorus atoms. Also, the resonance for the methyne hydrogen atom shows a splitting pattern of a doublet of doublet of triplet at δ 7.29 in the ^{1}H NMR spectrum, which confirms the proximity of the methyne hydrogen and the hydride atoms ($^{3}J_{H-H}$ = 2.6 Hz) in the structure of **3l**.

Addition of CF_3H to **2** led to decomposition after 3 days at ambient temperature. No evidence for the formation of a C−H activation product could be found by ^{1}H, ^{31}P{^{1}H}, and ^{19}F NMR spectroscopy. The failure to cleave a C−H bond in CF_3H was also observed in the [Tp′Rh(CNneopentyl)] system[35] and can be explained on the basis that the steric hindrance of three fluorine atoms disfavors the formation of an alkane σ-complex.[39,42]

dx.doi.org/10.1021/ja4080985 | J. Am. Chem. Soc. 2013, 135, 16198−16212

While **3a** is stable enough in air to obtain complete characterization and the crystal structure has been reported previously,[37] the further structural knowledge of other Tp′Rh(PMe$_3$)(R)H complexes is built upon the crystallographic analysis of the halo-derivatives **4** (Figure 4). Except for the difficulty to grow qualified single crystals for **4b**, the structures of **4c**−**4i** contain a general octahedral geometry around the rhodium center. The κ^3-coordination of the Tp′ ligand is reasonable for a Rh(III) complex.

Photolysis of 1 in Selected Terminal Alkynes. As shown in eq 8, irradiation works much better for aliphatic alkynes

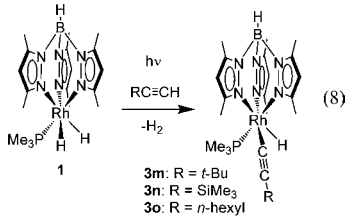

(8)

versus aryl alkynes, because short photolysis times are required and the reactions are both clean and regioselective. Irradiation of **1** in neat 3,3-dimethyl-1-butyne for 20 min afforded the clean formation of colorless Tp′Rh(PMe$_3$)(C≡C-*t*-Bu)H (**3m**), which contains a hydride resonance at δ −16.49 (dd, $^1J_{Rh-H}$ = 20.7 Hz, $^2J_{P-H}$ = 30.0 Hz) in the ^{1}H NMR spectrum. Photolysis of **1** in ethynyltrimethylsilane resulted in the clean formation of Tp′Rh(PMe$_3$)(C≡CSiMe$_3$)H (**3n**) with a hydride resonance at δ −16.12 (dd, $^1J_{Rh-H}$ = 21.0 Hz, $^2J_{P-H}$ = 29.4 Hz). Unlike the reaction with Tp′Rh(CNneopentyl),[33] no activation of the Si-methyl C−H bond was observed in this reaction. The analogous photolysis of **1** in 1-octyne also gave only one type of hydrido species, which is assigned as Tp′Rh(PMe$_3$)(C≡C-*n*-hexyl)H (**3o**). The hydride resonance appears as a doublet in the ^{1}H NMR spectrum at δ −16.48 (dd, $^1J_{Rh-H}$ = 20.8 Hz, $^2J_{P-H}$ = 30.0 Hz). No other isomers from activation of primary or secondary sp^3 C−H bonds were observed in this reaction. For aryl alkynes, much longer irradiation times are required to consume **1**, and decomposition of starting material or product or both occurs during irradiation.

Thermolysis of 2 in Terminal Alkynes. Compared with photolysis, thermal exchange with **2** is more feasible with arylalkyne substrates offering a milder reaction environment. Reaction of **2** with 4-ethynylanisole shows a high conversion to **3p** with traces of aryl activation products. However, exchange of **2** with 3,3,3-trifluoro-1-propyne, phenylacetylene, and 4-ethynyl-*α*,*α*,*α*-trifluorotoluene at room temperature gives a mixture of η^2-alkyne intermediates as well as the hydride-containing products (Scheme 2).

The η^2-alkyne intermediates were kinetically favored but thermally less stable than the corresponding hydrido species. For example, **3q**-η^2 dominated in the initial product distribution (within 1 day) in activation of 3,3,3-trifluoro-1-propyne. No obvious growth of **3q** was detected after a longer time (up to 6 days) at ambient temperature. Therefore, the solid residue was dissolved in C_6D_6 and heated at 140 °C to hasten the isomerization from **3q**-η^2 to **3q**. Conversion from **3q**-η^2 to **3q** was observed by ^{1}H and ^{31}P{^{1}H} NMR spectroscopy. Compound **3q**-η^2 disappeared after heating for 5 h, and only a small portion of benzene activation product was formed, which suggested that the isomerization between **3q**-η^2 and **3q** proceeds by an intramolecular pathway. Similar results were

Scheme 2. Exchange of 2 with Terminal Alkynes

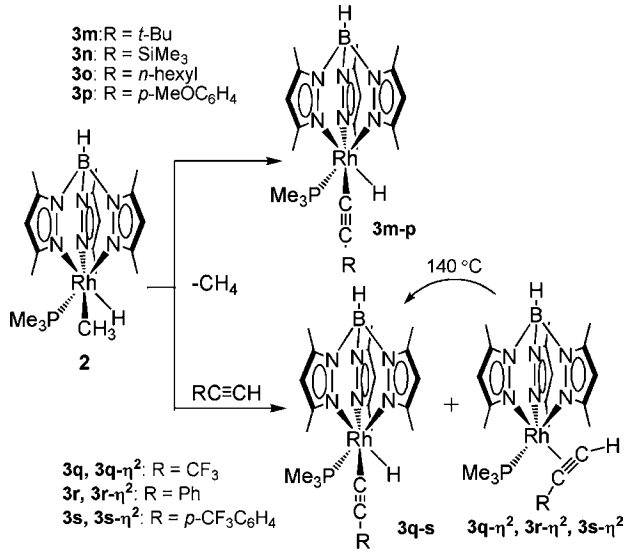

found by NMR spectroscopy in the activation of phenylacetylene and 4-ethynyl-*α*,*α*,*α*-trifluorotoluene (Figure 5).

The ^{11}B NMR resonances of **3q**-η^2 appeared at δ − 8.65 and the IR spectrum displays a band at 2530 cm^{-1}, both indicating κ^3-hapticity of the Tp′ ligand.[43] The molecular structure of **3q**-η^2 was further determined by X-ray crystallographic analysis of qualified crystals grown in ether (Figure 6). The thermodynamic stability of **3m**−**o** and **3q**,**r** enables direct crystallization of the hydridic species. These structures have typical Rh−C(sp) distances of 1.954−1.987 Å and C(sp)-C(sp) distances of 1.162−1.218 Å.

Reductive Elimination of Tp′Rh(PMe$_3$)(R)H. The disappearance rates of Tp′Rh(PMe$_3$)(R)H to eliminate RH in C_6D_6 have been measured by ^{1}H NMR spectroscopy and follow first-order kinetics to completion, forming **3a** as seen with Tp′Rh(CNR)(R)H. Table 1 summarizes the rate constants at 30 °C and the calculated activation barriers $\Delta G^{\ddagger}_{re}$. The rate of reductive elimination of RH from Tp′Rh(PMe$_3$)(R)H is *faster* than that from Tp′Rh(CNneopentyl)(R)H (e.g., $t_{1/2}$ = 1.0 h for reductive elimination of benzene from Tp′Rh(PMe$_3$)(C_6H_5)H versus $t_{1/2}$ = 3.6 h for Tp′Rh(CNneopentyl)(C_6H_5)H[10] at 100 °C). The kinetics of **3a** reductive elimination were conducted at varied temperatures (90−120 °C) to give the overall activation parameters of $\Delta H^{\ddagger}$ = 32.6 ± 3.3 kcal mol^{-1} and $\Delta S^{\ddagger}$ = 10.9 ± 0.2 eu. Low temperature NMR spectroscopy is required to monitor the rates of reductive elimination of **3g** and **3h**. Compound **3g** decomposes in pentane after overnight incubation, and decomposition of **3h** in cyclopentane occurs within hours. In contrast, however, the rates of elimination of alkynes from Tp′Rh(PMe$_3$)(C≡CR)H (**3m**−**s**) are much *slower* than the rates from Tp′Rh(CNR)(C≡CR)H (Table 2). These experiments for alkyne reductive elimination were performed at 140 °C to observe obvious consumption of the complexes **3m**−**s** in reasonable times. As mentioned previously,[37] the formation of rhodium(I) bisphosphine complex Tp′Rh(PMe$_3$)$_2$ was also observed at this temperature, which is attributed to the lability of Tp′Rh(PMe$_3$)(C_6D_5)D above 100 °C. Only a small portion of the complexes was converted to Tp′Rh(PMe$_3$)(C_6D_5)D, but the growth of Tp′Rh(PMe$_3$)(C_6F_5)H in experiments in which

dx.doi.org/10.1021/ja4080985 | J. Am. Chem. Soc. 2013, 135, 16198−16212

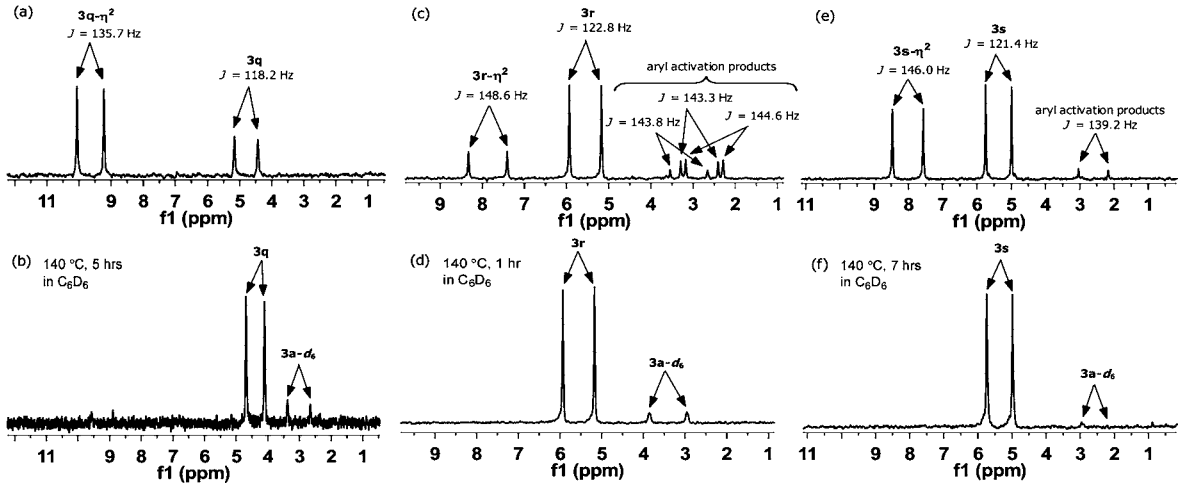

Figure 5. $^{31}P\{^{1}H\}$ NMR resonances of activation products formed by reductive elimination of methane from **2**: activation of 3,3,3-trifluoro-1-propyne (a) after 1 day at RT and (b) after heating at 140 °C in C_6D_6 for 5 h; activation of phenylacetylene (c) after 1 day at RT and (d) after heating at 140 °C in C_6D_6 for 1 h; activation of 4-ethynyl-α,α,α-trifluorotoluene (e) after 1 day at RT and (f) after heating at 140 °C in C_6D_6 for 7 h.

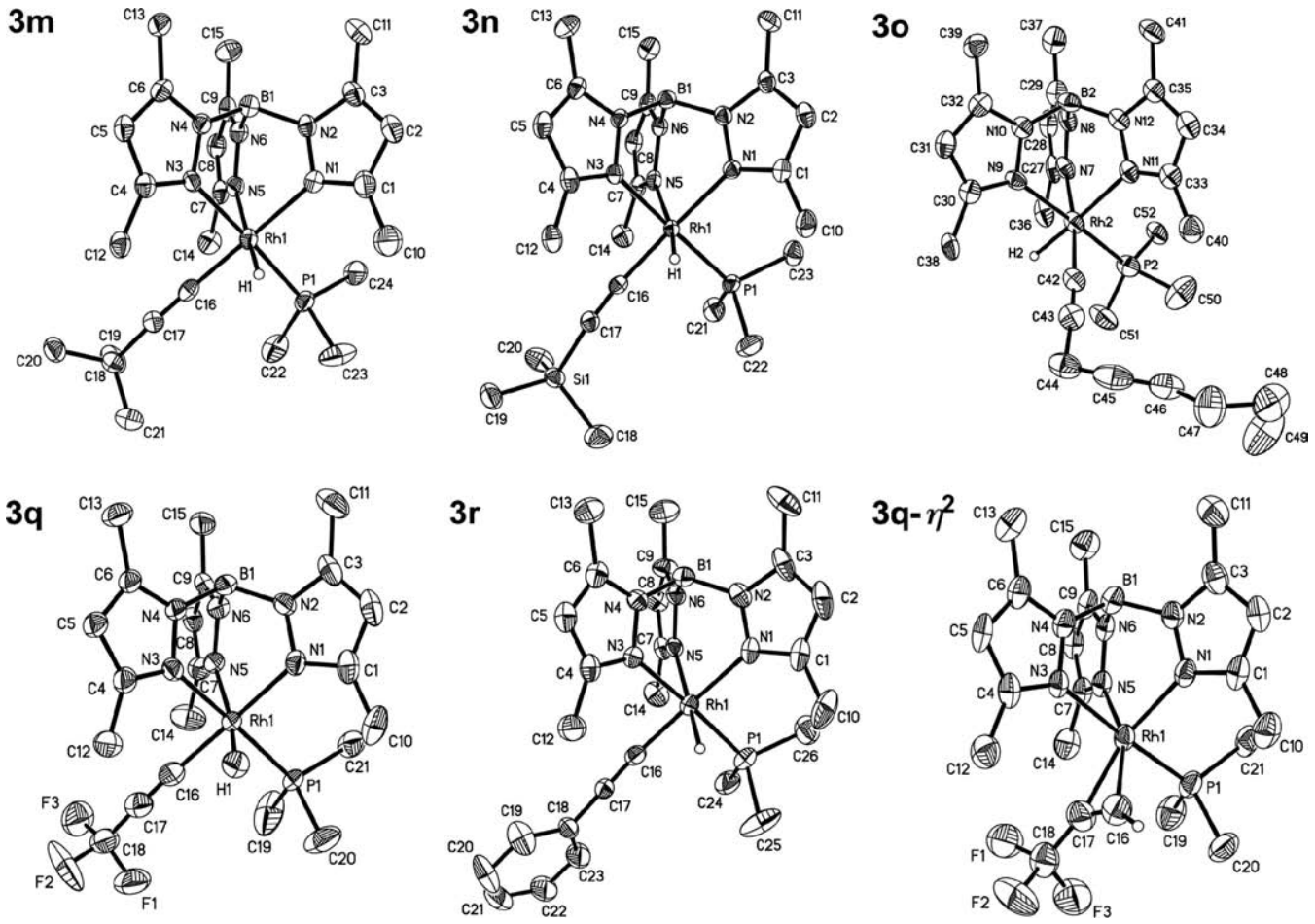

Figure 6. Thermal ellipsoid drawings of **3m**−**o**, **3q**,**r** and **3q**-η^2. Ellipsoids are shown at the 50% probability level, and hydrogen atoms have been omitted for clarity.

pentafluorobenzene had been added suggests a lower barrier for RH reductive elimination than other decomposition pathways.

One exception in the kinetic study is that the measurement of reductive elimination of **3e** was not realized because the intramolecular isomerization occurs prior to the trapping by C_6D_6 (eq 9). Heating the complex **3e** in C_6D_6 after a week gave a π-coordinated intermediate $Tp'Rh(PMe_3)(\eta^2\text{-}CH_3C{\equiv}CCH_3)$ (**7**) with only a small quantity of **3a**-d_6 (<5%). The isomerization followed first-order kinetics with $t_{1/2}$ = 38.1 h at 30.0 °C. The process ultimately resulted in complete conversion of **7** to **3a**-d_6 after 1 month. The occurrence of **7** suggests that π-electron donation from bound 2-butyne to the

dx.doi.org/10.1021/ja4080985 | J. Am. Chem. Soc. 2013, 135, 16198−16212

Table 1. Rates of Reductive Elimination of RH from Tp′Rh(PMe$_3$)(R)H in C$_6$D$_6$[a]

RH	T, °C	k_{re}(RH), s^{-1}	$\Delta G^{\ddagger}_{re}$, kcal mol^{-1}
benzene	30	4.45(4) × 10^{-9}[b]	29.34(1)
methane	30	3.35(2) × 10^{-4}	22.58(1)
mesitylene	30	6.37(3) × 10^{-4}	22.19(1)
3,3-dimethyl-1-butene	30	4.23(12)× 10^{-8}	27.99(2)
2-methoxy-2-methylpropane	30	1.89(5) × 10^{-6}	25.70(2)
acetone	30	3.77(4) × 10^{-7}	26.67(1)
pentane	9	3.01(3) × 10^{-4}	21.00(1)
c-pentane	−2	2.35(6) × 10^{-4}	20.34(1)
α,α,α-trifluoroethane	30	1.24(4) × 10^{-6}	25.95(2)
fluoromethane	67	2.37(4) × 10^{-6}	28.75(1)
dimethyl ether	30	6.78(22) × 10^{-7}	26.31(2)
difluoromethane	100	5.85(72) × 10^{-6}	30.95(9)

[a]Errors are reported as standard deviations. Errors in $\Delta G^{\ddagger}_{re}$ are calculated from k as propagated errors, using $\sigma_G = -(RT/k_{re})\sigma_k$. The errors are small because G is a log function of rate. Systematic errors are probably larger and can be estimated as ±0.1 kcal mol^{-1} assuming 10% error in k. [b]Rate constant calculated from Eyring plot data in Supporting Information.

Table 2. Rates of Reductive Elimination of RC≡CH from Tp′Rh(PMe$_3$)(C≡CR)H in C$_6$D$_6$ at 140 °C[a]

RC≡CH	k_{re}(RH), s^{-1}	$\Delta G^{\ddagger}_{re}$, kcal·mol^{-1}
3,3-dimethyl-1-butyne	2.86(6) × 10^{-6}	34.94(2)
ethynyltrimethylsilane	1.26(3) × 10^{-7}	37.50(2)
1-octyne	6.14(22) × 10^{-6}	34.31(3)
4-ethynylanisole	9.56(32) × 10^{-7}	35.83(3)
3,3,3-trifluoro-1-propyne	3.97(10) × 10^{-7}	36.56(2)
phenylacetylene	3.17(20) × 10^{-6}	34.85(5)
4-ethynyl-*α,α,α*-trifluorotoluene	7.72(10) × 10^{-7}	36.01(1)

[a]Errors are reported as standard deviations. Errors in $\Delta G^{\ddagger}_{re}$ are calculated using $\sigma_G = -(RT/k_{re})\sigma_k$. Systematic errors are probably larger and can be estimated as ±0.1 kcal mol^{-1} assuming 10% error in k.

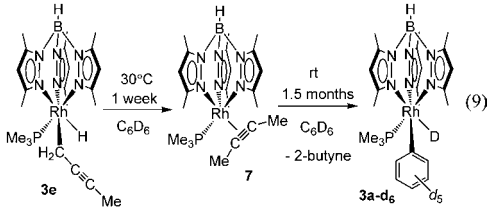

active fragment Tp′Rh(PMe$_3$) is more kinetically favorable than dissociation of the alkyne. The lack of a clean reductive elimination precludes use of data from **3e** for Rh−C bond strength determination.

The structure of **7** was initially inferred on the basis of several observations: (1) The ^{1}H NMR signals of Tp′ suggest the 2:1 symmetry of Pz′ rings, and 3 methyl resonances of area 6H are seen along with 2 methyl resonances of area 3H. Thus a structure with planar symmetry for Tp′ ligand and coordinated 2-butyne is plausible. (2) The ^{11}B NMR resonance (δ −8.31) and IR vibration of the B−H stretch (ν 2543 cm^{-1}) suggest a typical κ^3-Tp′ coordination at the rhodium center.[31,32] (3) A trigonal bipyramid structure has been found in the X-ray structure of (κ^3-Tp′)Rh(CN-2,6-xylyl)(η^2-C$_2$H$_4$), which is used to support similar coordination geometries in other derivatives (κ^3-Tp′)Rh(CNneopentyl)(η^2-C$_2$H$_4$) and (κ^3-Tp′)Rh(CNneopentyl)(η^2-MeCH=CH$_2$), which display consistent ^{11}B NMR and IR data.[31,32,42] The X-ray analysis of **7** unambiguously confirms the κ^3-coordination of Tp′, as well as the distorted octahedral symmetry with an η^2-bound 2-butyne (Figure 7). The C16−C17 distances of 1.275(10) Å (cf.

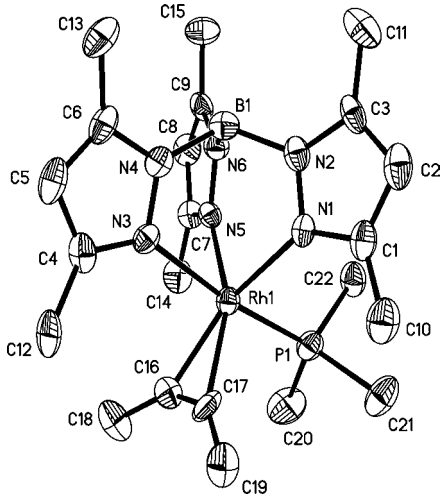

Figure 7. Thermal ellipsoid drawing of Tp′Rh(η^2-C$_2$Me$_2$)(PMe$_3$) (**7**). Ellipsoids are shown at the 50% probability level, and hydrogen atoms have been omitted for clarity.

d(C≡C) of 1.182 Å in free 2-butyne) as well as related angles of the coordinated 2-butyne (C(17)−C(16)−C(18) = 146.1(8)° and C(16)−C(17)−C(19) = 143.9(8)°) suggest that strong back-donation from the metal decreases the bond order from sp to nearly sp^2. It is interesting to note that **7** was not observed in the exchange reaction of **2** with 2-butyne, which indicates that C−H bond cleavage is kinetically preferred over π-complexation. The existence of a π-bound intermediate is not seen with the [Tp′Rh(CNneopentyl)] fragment, where reductive elimination of Tp′Rh(CNneopentyl)(CH$_2$C≡CMe)H in C$_6$D$_6$ yielded only Tp′Rh(CNneopentyl)(C$_6$D$_5$)D, and η^2-coordinated alkynes were not observed in any alkyne activation. This difference implies the necessity of a more electron-rich [Tp′Rh(L)] system (L = phosphine versus isonitrile) to stabilize the π-bound adduct with a stronger back-donation from the metal center to the triple bond.

Competitive Selectivity Experiments. Photolyses of Tp′Rh(PMe$_3$)H$_2$ in a mixture of two substrates were conducted at low temperature to measure the competitive selectivity for C−H activation of various substrates. The samples were irradiated for a short time to avoid the interconversion between hydridic products and the late-stage decomposition. The ratio of the two substrates was measured by ^{1}H NMR analysis before irradiation, and the product distribution was determined on the basis of the relative areas of the corresponding resonances by ^{1}H NMR spectroscopy in deuterated solvent (C$_6$D$_6$ or C$_6$D$_{12}$) (see Supporting Information for details). The relative competitive rates, $k_{benzene}/k_{substrate}$, are reported in Table 3, as well as the selectivity data for C−H activation at the [Tp′Rh(CNneopentyl)] fragment.

The order of kinetic selectivities for various C−H bonds could be seen to follow the trend: terminal alkynes > arenes > primary C−H bonds> olefins > secondary C−H bonds. These results suggest that the kinetic selectivity closely follows the C−H bond strengths. The type of α-functional group influences

dx.doi.org/10.1021/ja4080985 | J. Am. Chem. Soc. 2013, 135, 16198−16212

Table 3. Kinetic Selectivity Data

run	substrates	T (°C)	$k_{benzene}/k_{substrate}$ [a] Tp′Rh(PMe_3)	$k_{benzene}/k_{substrate}$ [b] Tp′Rh(CNneopentyl)
1	methane	−10	2.55(13)[c]	3.31(17)
2	mesitylene	−10	1.36(7)	1.28(19)
3	3,3-dimethyl-1-butene	10	4.39(22)	10.2(15)
4	acetone	−10	6.44(32)	3.71(19)
5	2-methoxy-2-methylpropane	−10	3.51(18)	4.53(23)
6	*n*-pentane	−10	2.45(12)	4.64(67)
7	cyclopentane	−10	16.0(8)	31.9(48)
8	CH_3CF_3	10	5.03(25)	18.2(9)
9	CH_3F	10	1.06(5)	4.24(21)
10	dimethyl ether	10	1.82(9)	2.33(12)
11	CH_2F_2	10	0.63(3)	62.9(31)
12	3,3-dimethyl-1-butyne	10	1.72(9)	5.49(83)
13	ethynyltrimethylsilane	10	1.61(8)	3.00(45)
14	1-octyne	10	1.88(9)	8.31(125)
15	3,3,3-trifluoro-1-propyne	−10	0.23(1)	3.80(13)
16	4-ethynylanisole	10	1.65(8)	1.66(25)
17	phenylacetylene	10	2.14(11)	2.42(36)
18	4-ethynyl-α,α,α-trifluoro-toluene	10	0.92(5)	0.85(13)

[a]Errors in rate ratio estimated at 5% for proton NMR integration; The relative rates $k_{benzene}/k_{substrate}$, at which the unsaturated fragment Tp′Rh(PMe_3) reacts with two types of C−H bonds could be calculated in $k_{benzene}/k_{substrate} = (I_{benzene}/I_{substrate})(n_{substrate}/n_{benzene})$. See Supporting Information for calculation details. [b]Data from refs 33−35. [c]$k_{benzene}/k_{methane} = (k_{benzene}/k_{pentane})(k_{pentane}/k_{methane}) = 2.45 \times 1.04 = 2.55$.

activation selectivities for sp^3 C−H bonds at least as much as the C−H bond strength. This assertion is difficult to determine due to the small range of bond strengths investigated.

However, within the narrow range of sp^3 C−H bond strengths, the inconsistency of selectivities versus C−H bond energies indicates that α-functional groups also influence activation selectivities. Compared with the case of the [Tp′Rh(CNR)] fragment, the intermolecular kinetic selectivity of [Tp′Rh(PMe_3)] is generally smaller with a few exceptions.

Thermodynamics of C−H Activation: Relative Rh−C versus C−H Bond Strengths. The relative Rh−C bond strengths were calculated from the above kinetic data as indicated in Figure 1.[35] The competitive free energy differences can be determined as indicated in eq 10 (see Table 4), and the overall driving force, ΔG°, using eq 11. Using these measured values along with known C−H bond strengths, the relative Rh−C bond energies of the C−H activation complexes can be determined using eq 12, which includes the assumption that $\Delta G^\circ = \Delta H^\circ - RT\ln(H/H')$, where H/H' is the ratio of the number of hydrogen atoms on the substrates to account for the statistical (entropic) contribution to the free energy.[37]

$$\Delta\Delta G^{\ddagger}_{oa} = -RT\ln(k/k') \tag{10}$$

$$\Delta G^\circ = \Delta G^{\ddagger}_{re}(\mathrm{R'H}) + \Delta\Delta G^{\ddagger}_{oa} - \Delta G^{\ddagger}_{re}(\mathrm{RH}) \tag{11}$$

$$\begin{aligned} D_{rel}(\mathrm{Rh{-}C}) &= [\Delta H(\mathrm{Rh{-}R}) - \Delta H(\mathrm{Rh{-}R'})] \\ &= -\Delta G^\circ + RT\ln(H/H') + [\Delta H(\mathrm{R{-}H}) \\ &\quad - \Delta H(\mathrm{R'{-}H})] \end{aligned} \tag{12}$$

A plot of D_{rel}(M−C) versus D(C−H) for the unsubstituted hydrocarbons shows a linear correlation with a slope of 1.54, which is ∼10% larger than the slope (1.38) for Tp′Rh(CNneopentyl).[33] The value of $R_{M-C/C-H}$ also suggests an even larger preference for activation of strong C−H bonds by [Tp′Rh(PMe_3)] than by [Tp′Rh(CNR)], which will produce more robust Rh−C bonds (54% stronger) (solid line, Figure 8).[45] As inspired from previous work in the [Tp′Rh(CNneopentyl)] system, the effect of substitution on strengthening D_{rel}(M−C) was examined among Tp′Rh(PMe_3)(CH_2X)H derivatives as well (dashed line, Figure 8). The relative Rh−CH_2X bond energies of this group correlate well with the corresponding H−CH_2X bond energies. The slope of 1.71 is larger than that for the parent hydrocarbons and the

Table 4. Kinetic and Thermodynamic Data for Formation of Tp′Rh(PMe_3)(R)H

R	D(C−H)[a]	$\Delta\Delta G^{\ddagger}_{oa}$ [b,c]	ΔG° [b]	D_{rel}(Rh−R)[b]
phenyl	112.9	0.00	0.00(5)	0
^{t}butylvinyl	111.1	0.83(3)	2.19(5)	−2.9
methyl	105.0	0.49(3)	7.25(3)	−14.9
n-pentyl	100.2	0.47(3)	9.04(4)	−21.7
c-pentyl	95.6	1.45(3)	10.80(4)	−28.4
$CF_3C{\equiv}C$	135.4	−0.77(3)	−9.18(5)	32.7
n-hexylC≡C	131.0	0.36(3)	−5.81(6)	25.0
$SiMe_3C{\equiv}C$	131.6	0.27(3)	−9.09(5)	28.8
^{t}BuC≡C	131.4	0.31(3)	−6.49(5)	26.0
PhC≡C	133.2	0.43(3)	−6.28(8)	27.6
p-$CF_3C_6H_4C{\equiv}C$	127.8	−0.05(3)	−7.91(4)	23.9
p-$MeOC_6H_4C{\equiv}C$	122.7	0.28(3)	−7.40(6)	18.3
mesityl	89.4	0.16(3)	7.31(3)	−31.1
$CH_3C(=O)CH_2$	96.0	0.97(3)	3.65(4)	−20.5
CH_2O^tBu	93.0[d]	0.66(3)	4.30(5)	−23.8
CH_3OCH_2	96.1	0.34(3)	3.37(5)	−20.2
CH_2F	101.3	0.03(3)	0.22(4)	−11.4
CHF_2	103.2	−0.26(3)	−2.63(12)	−6.4
CH_2CF_3	106.7	0.91(3)	4.30(5)	−10.1

[a]Hydrocarbon C−H bond strengths are from experimental data.[44] Alkyne C−H bond strengths were calculated using B3LYP/6-31G**.[31] [b]All values are in kcal·mol^{-1}, and a positive value denotes that benzene is kinetically favored. Systematic errors are probably larger and can be estimated as ±0.1 kcal mol^{-1} [c]Errors in rate ratio estimated at 5%, giving $\sigma_G = -(RT/\mathrm{ratio})\sigma_{ratio} = 0.05RT \approx 0.03$ kcal·mol^{-1}. [d]The value of methyl ethyl ether was used instead because the bond strength for methyl *t*-butylether is not experimentally known.

dx.doi.org/10.1021/ja4080985 | J. Am. Chem. Soc. 2013, 135, 16198−16212

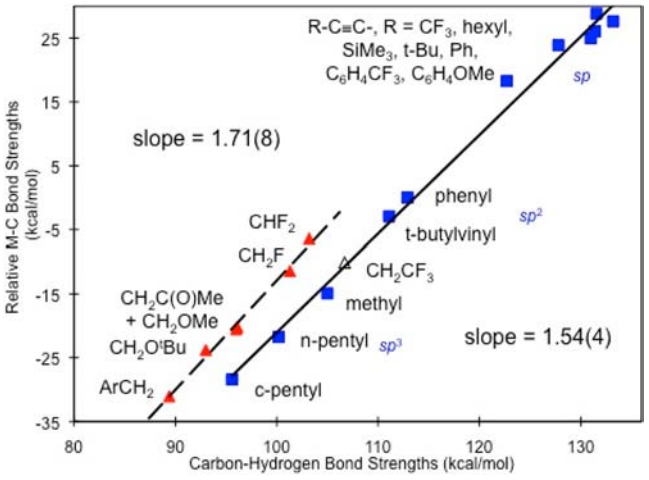

Figure 8. Plot of relative experimental M−C bond strengths vs C−H bond strengths for Tp′Rh(PMe$_3$)(R)H. The solid line is fit to the α-unsubstituted hydrocarbons (blue ■, $y = 1.543x - 175.3$), and the dashed line is fit to the $-CH_2X$ substrates and $-CHF_2$ (red ▲, $y = 1.712x - 184.1$). $-CH_2CF_3$ is also shown but not included in either fit. Experimental C−H bond strengths were used for all substrates except the alkynes. Alkyne C−H bond strengths were calculated (B3LYP) since experimental values are unavailable.[33] The vertical separation of the lines at D_{C-H} = 100 kcal mol^{-1} is 8.1 kcal mol^{-1}.

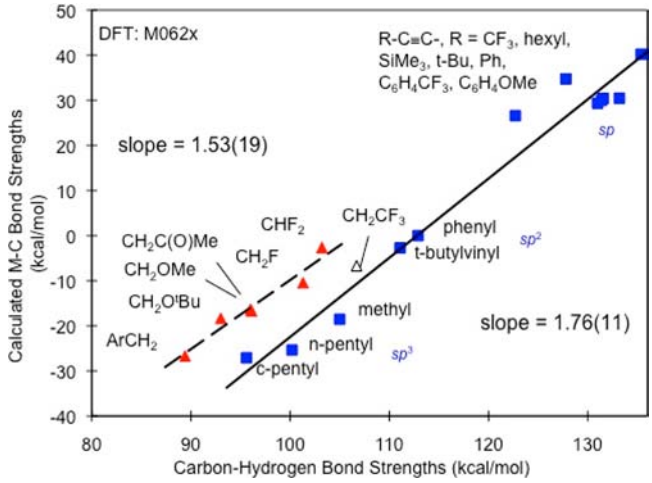

Figure 9. DFT calculated plot of relative M−C bond strengths vs C−H bond strengths for Tp′Rh(PMe$_3$)(R)H. The lower line is fit to the hydrocarbons (blue ■, $y = 1.531x - 162.9$), and the upper line is fit to the $-CH_2X$ and CHF_2 substrates (red ▲, $y = 1.756x - 198.0$). Data for CH_3CF_3 activation is also shown, but not included in the fits. M06-2X method and basis set 6-31G** for first row atoms and pseudopotentials; additional functions optimized by Stuttgart group for atoms beyond the second row. Experimental C−H bond strengths were used for all substrates except the alkynes. Alkyne C−H bond strengths were calculated (B3LYP) since experimental values are unavailable.[33] The vertical separation of the lines at D_{C-H} = 100 kcal mol^{-1} is 12.6 kcal mol^{-1}.

bond energies are increased vertically by +8.1 kcal/mol, which is slightly larger than that in the Tp′Rh(CNneopentyl)(R)H system (+7.5 kcal/mol). While the Rh−CH_2X bonds (X = aryl, keto, and alkoxy) are weakened compared with the Rh−CH_3 bond, fluorine substitution leads to stronger Rh−C bonds than Rh−CH_3 in the cases of CH_3F, CH_2F_2, and CH_3CF_3. As discussed in the isocyanide system, the weakened Rh−CH_2X bonds are actually stronger than expected on the basis of the weak H−CH_2X bonds that are broken. The origin of the strengthening of the M−CH_2X bonds can be explained in terms of hyperconjugation with the π-system in the arene of mesitylene and C═O of acetone or with the CH_2−X σ^* orbitals when X = OR or F. A greater ionic contribution to the M−CH_2X bond due to inductive effects may also play a role. The effect of substitution stabilization is quantitatively measured based on the difference of the experimental data and that extrapolated from the fit of the parent hydrocarbons. The relative Rh−mesityl bond is 6.3 kcal/mol stronger than its corresponding value calculated from the hydrocarbon correlation trendline. The effect of the carbonyl in acetone raises D_{rel}(Rh−C) by 6.7 kcal/mol; *t*-butyl methyl ether and dimethyl ether increase their related M−C bond energies by 8.1 and 6.9 kcal/mol, respectively; D_{rel}(Rh−CH_2F) and D_{rel}(Rh−CHF_2) were also strengthened by 7.6 and 9.7 kcal/mol, respectively. As expected, β-fluorine substitution only slightly stabilize the Rh−CH_2CF_3 bond by 0.6 kcal/mol.

In addition, DFT calculated Rh−C bond energies using Tp′Rh(PMe$_3$)(R)H as a model show similar trends versus C−H bond energies (Figure 9). The calculated slope of the "normal" hydrocarbons is 1.76, which is larger than the experimental result by 14%. However for the substituted substrate, the slope value was underestimated by 11%. A similar "overestimation" of the DFT calculated slope was noted for the Tp′Rh(CNMe)(R)H complexes. For comparison, Landis has calculated $R_{M-C/C-H}$ values for sp, sp^2, and sp^3 hydrocarbyls of all transition metals in model complexes H_nM−R, which ranged from 1.20 to 1.86.[46] Also, as mentioned earlier, Eisenstein and Perutz calculated slopes for fluoroarene activation in [CpRe(CO)L], [CpRhL], and [CpIrL] (L = CO, PH$_3$) that were 10−20% larger for L = PH$_3$ than for L = CO,[38] in agreement with the experimental effects seen here for exchange of CNR by PMe$_3$.

■ CONCLUSIONS

Tp′Rh(PMe$_3$)(CH$_3$)H is a good precursor to produce the active fragment [Tp′Rh(PMe$_3$)], which efficiently inserts into C−H bonds in various types of hydrocarbons. The highly selective C−H activation ensures the clean formation of the target product. Both experimentally measured and DFT calculated relative Rh−C bond strengths correlate well with corresponding C−H bond strengths to give two separate linear correlations based on having α-substitution. The slopes (1.71, 1.54) are generally larger than that in Tp′Rh(CNneopentyl)(R)H (1.40, 1.38), indicative of the effect of replacement of a π-acceptor isonitrile with a σ-donating phosphine. Compared with the parent methane, fluoromethane, difluoromethane, and 1,1,1-trifluoroethane all strengthen the resulting Rh−C bonds by 3.5, 8.5, and 4.8 kcal/mol over Rh−CH_3, while other substituted substrates all weaken the Rh−C bonds by 5.3−16.2 kcal/mol versus Rh−CH_3. Nevertheless, the M−CH_2X bonds were still strengthened by substitution based upon what was expected from the correlations of the parent hydrocarbons with the corresponding C−H bond strengths.

■ EXPERIMENTAL SECTION

General Procedure. All operations and routine manipulations were performed under a nitrogen atmosphere, either on a high-vacuum line using modified Schlenk techniques or in a Vacuum Atmospheres Corp. Dri-Lab. Benzene-d_6 was distilled under vacuum from a dark purple solution of benzophenone ketyl and stored in an ampule with a Teflon valve. Cyclopentane, THF-d_8, cyclohexane-d_{12}, mesitylene, 3,3-

dx.doi.org/10.1021/ja4080985 | J. Am. Chem. Soc. 2013, 135, 16198−16212

dimethyl-1-butene, 2-methoxy-2-methylpropane, and terminal alkynes were dried over CaH_2 and vacuum-distilled prior to use. Acetone and 2-butyne were dried over potassium carbonate and vacuum-distilled prior to use. Other solvents were used directly from an Innovative Technologies PS-MD-6 solvent system. All the gases were purchased from Matrix Scientific, Synquest Laboratories, and Aldrich Chemical Co. and used straight from lecture bottles. Preparations of Tp′Rh(PMe$_3$)Cl$_2$, Tp′Rh(PMe$_3$)H$_2$ (**1**), and Tp′Rh(PMe$_3$)(C$_6$H$_5$)H (**3a**) have been previously reported.[40,47]

All ^{1}H, ^{13}C{^{1}H}, ^{19}F, and ^{31}P{^{1}H} NMR spectra were recorded on a Bruker Avance 400 or 500 MHz NMR spectrometer. All ^{1}H chemical shifts are reported in ppm (δ) relative to the chemical shift of residual solvent (benzene-d_6 (δ 7.16), C_6D_{12} (δ 1.40), THF-d_8 (δ 3.58), or $CDCl_3$ (δ 7.26)). ^{11}B{^{1}H} were referenced to external $BF_3{\cdot}OEt_2$ in THF-d_8 (δ 0.0). ^{13}C{^{1}H} were referenced to benzene-d_6 (δ 128.0), THF-d_8 (δ 67.4), C_6D_{12} (δ 27.2), or $CDCl_3$ (δ 77.2). ^{19}F NMR spectra were referenced to external α,α,α-trifluorotoluene in cyclohexane-d_{12} (δ 0.0). ^{31}P{^{1}H} NMR spectra were referenced to external H_3PO_4 (δ 0.0). IR spectra were recorded in the solid state on a Nicolet 4700 FTIR spectrometer between 4000 and 600 cm^{-1}. All photolysis experiments were carried out using a water-filtered 200 W Hg−Xe lamp and filtered using a 270−370 nm band-pass filter. Silica gel was heated overnight at 200 °C and then stored under nitrogen prior to use. A Bruker-AXS SMART platform diffractometer equipped with an APEX II CCD detector was used for X-ray crystal structure determination.

Preparation of Tp′Rh(PMe$_3$)(CH$_3$)Cl (2-Cl). To a stirred solution of 55 mg (0.101 mmol) of Tp′Rh(PMe$_3$)Cl$_2$ in 7 mL of THF was added dropwise 38 μL (0.11 mmol) of 3 M CH_3MgCl solution in THF. The color changed from orange-yellow to yellow upon addition of the Grignard reagent. After the reaction mixture was stirred for 15 min, the solution was quenched with a saturated solution of NH_4Cl(aq) until the solution was clear again. The volatiles were removed under vacuum. The solids were mixed with 5 mL of methylene chloride and filtered through Celite to give a clear yellow solution, which was layered with hexane for recrystallization. Yellow crystals (52 mg, 98%) were collected and dissolved in C_6D_6. ^{1}H NMR (500 MHz, C_6D_6): δ 1.10 (d, $^2J_{P-H}$ = 10.3 Hz, 9H, PMe$_3$), 1.99 (s, 3H, pzCH$_3$), 2.12 (s, 3H, pzCH$_3$), 2.19 (s, 3H, pzCH$_3$), 2.28 (dd, $^2J_{Rh-H}$ = 2.2 Hz, $^3J_{P-H}$ = 3.0 Hz, 3H, Rh-CH$_3$), 2.30 (s, 3H, pzCH$_3$), 2.72 (s, 3H, pzCH$_3$), 2.89 (s, 3H, pzCH$_3$), 5.48 (s, 1H, pzH), 5.51 (s, 1H, pzH), 5.72 (s, 1H, pzH). ^{13}C{^{1}H} NMR (500 MHz, C_6D_6): δ −0.19 (dd, $^1J_{Rh-C}$ = 9.2 Hz, $^2J_{P-C}$ = 20.5 Hz, RhCH$_3$), 12.72 (s, pzCH$_3$), 12.94 (s, pzCH$_3$), 13.36 (s, pzCH$_3$), 14.24 (s, pzCH$_3$), 15.78 (d, $^1J_{P-C}$ = 33.3 Hz, P(CH$_3$)$_3$), 16.14 (s, pzCH$_3$), 16.37 (s, pzCH$_3$), 108.09 (d, $^4J_{P-C}$ = 4.4 Hz, pzCH), 108.42 (s, pzCH), 109.03 (s, pzCH), 142.41 (d, $^4J_{P-C}$ = 2.4 Hz, pzCq), 143.96 (s, pzCq), 144.65 (s, pzCq), 151.79 (s, pzCq), 152.21 (d, $^3J_{P-C}$ = 4.3 Hz, pzCq), 153.16 (s, pzCq). ^{31}P{^{1}H} NMR (400 MHz, C_6D_6): δ 2.50 (d, $^1J_{Rh-P}$ = 128.3 Hz). Anal. Calcd for $C_{19}H_{34}BClN_6PRh$ C, 43.33; H, 6.51; N, 15.96. Found: C, 43.45; H, 6.47; N, 15.81.

Preparation of Tp′Rh(PMe$_3$)(CH$_3$)H (2). To a yellow solution of 40 mg (0.076 mmol) of Tp′Rh(PMe$_3$)(CH$_3$)Cl (**2**-Cl) in 2 mL of THF was added 26 mg (0. 12 mmol) of Cp_2ZrH_2. The suspension was stirred for 50 min at 18 °C and changed from light yellow to white. ^{1}H NMR (400 MHz, C_6D_6): δ −18.14 (dd, $^1J_{Rh-H}$ = 23.6 Hz, $^2J_{P-H}$ = 33.6 Hz, 1H, RhH), 0.98 (d, $^2J_{Rh-H}$ = 3.8 Hz, 3H, Rh-CH$_3$), 1.17 (d, $^2J_{P-H}$ = 9.0 Hz, 9H, PMe$_3$), 2.18 (s, 3H, pzCH$_3$), 2.18 (s, 3H, pzCH$_3$), 2.27 (s, 3H, pzCH$_3$), 2.32 (s, 3H, pzCH$_3$), 2.34 (s, 3H, pzCH$_3$), 2.52 (s, 3H, pzCH$_3$), 5.60 (s, 1H, pzH), 5.68 (s, 1H, pzH), 5.79 (s, 1H, pzH). ^{31}P{^{1}H} NMR (400 MHz, C_6D_6): δ 4.59 (d, $^1J_{Rh-P}$ = 147.7 Hz). A white crystalline solid was then isolated from the zirconium complexes by flash chromatography through silica gel in a pipet with a glass wool plug using 9:1 hexane−THF as the eluent (5× volume). Yield: 96% by ^{1}H NMR spectroscopy. Trace hydride resonances (4%) are attributable to Tp′Rh(PMe$_3$)(furanyl)H and Tp′Rh(PMe$_3$)(Cl)H.

*For Tp′Rh(PMe$_3$)(Cl)H (**5**).* ^{31}P{^{1}H} NMR (400 MHz, C_6D_6): δ 5.31 (d, $^1J_{Rh-P}$ = 122.0 Hz). See Supporting Information for details of its crystal structure. ^{1}H NMR resonances were reported previously.[40]

For Tp′Rh(PMe$_3$)(furanyl)H. ^{1}H NMR (400 MHz, C_6D_6), hydride resonances for two isomers: δ −17.66 (dd, $^1J_{Rh-H}$ = 22.9 Hz, $^2J_{P-H}$ = 31.5 Hz, 1H, RhH); −17.42 (dd, $^1J_{Rh-H}$ = 25.3 Hz, $^2J_{P-H}$ = 29.6 Hz, 1H, RhH).

Preparation of Tp′Rh(PMe$_3$)(R)H (3a−l): General Procedure. Ten milligrams (0.019 mmol) of **2**-Cl was used for the *in situ* synthesis of **2**, which was then dissolved in 0.4 mL of the corresponding RH and transferred to a resealable 5 mm NMR tube. After the reaction was complete at room temperature, the solvent was removed in vacuo, and the resulting residue was dissolved in C_6D_6. For activation of 1,1,1-trifluoroethane, fluoromethane, and difluoromethane, **2** was dissolved in 0.4 mL of C_6D_{12} and transferred to a high pressure medium wall NMR tube, followed by pressurization with the corresponding gas at 50 psi. ^{1}H, ^{11}B{^{1}H}, ^{13}C{^{1}H}, ^{19}F, and ^{31}P{^{1}H} NMR spectra were collected. The yields are almost quantitative except those for fluoromethane and difluoromethane.

*For Tp′Rh(PMe$_3$)(C$_6$H$_5$)H (**3a**).* Reaction was complete after overnight incubation. The volatiles were removed to give a pale yellow solid, which was dissolved in C_6D_6. ^{31}P{^{1}H} NMR (400 MHz, C_6D_6): δ 3.24 (d, $^1J_{Rh-P}$ = 145.8 Hz). ^{1}H NMR resonances were reported in ref 40.

*For Tp′Rh(PMe$_3$)(CH$_2$C$_6$H$_3$-3,5-(CH$_3$)$_2$)H (**3b**).* Reaction was complete after 2 d. The volatiles were removed to give a pale yellow solid, which was dissolved in C_6D_6. ^{1}H NMR (400 MHz, C_6D_6): δ −17.75 (dd, $^1J_{Rh-H}$ = 23.2 Hz, $^2J_{P-H}$ = 30.0 Hz, 1H, RhH), 1.01 (d, $^2J_{PH}$ = 9.2 Hz, 9H, PMe$_3$), 2.15 (s, 3H, pzCH$_3$), 2.22 (s, 3H, pzCH$_3$), 2.24 (s, 3H, pzCH$_3$), 2.31 (s, 6H, 2 × arylCH$_3$), 2.38 (s, 3H, pzCH$_3$), 2.52 (s, 3H, pzCH$_3$), 2.60 (s, 3H, pzCH$_3$), 3.16 (dt, $^2J_{H-H}$ = 12.0 Hz, $^2J_{Rh-H}$ = $^3J_{P-H}$ = 3.3 Hz, 1H, RhCH$_2$), 4.04 (dd, $^2J_{H-H}$ = 12.0 Hz, $^2J_{Rh-H}$ = 3.6 Hz, 1H, RhCH$_2$), 5.54 (s, 1H, pzH), 5.65 (s, 1H, pzH), 5.86 (s, 1H, pzH), 6.75 (s, 1H, arylH), 7.49 (s, 2H, 2arylH). ^{31}P{^{1}H} NMR (400 MHz, C_6D_6): δ 2.34 (d, $^1J_{Rh-P}$ = 150.7 Hz).

*For Tp′Rh(PMe$_3$)(CH═CHC(CH$_3$)$_3$)H (**3c**).* Reaction was complete after standing overnight. The volatiles were removed to give a white solid, which was dissolved in C_6D_6. ^{1}H NMR (400 MHz, C_6D_6): δ −17.05 (dd, $^1J_{Rh-H}$ = 24.9 Hz, $^2J_{P-H}$ = 32.3 Hz, 1H, RhH), 1.18 (s, 9H, C(CH$_3$)$_3$), 1.19 (d, $^2J_{PH}$ = 8.6 Hz, 9H, PMe$_3$), 2.13 (s, 3H, pzCH$_3$), 2.20 (s, 3H, pzCH$_3$), 2.27 (s, 3H, pzCH$_3$), 2.35 (s, 6H, 2 × pzCH$_3$), 2.56 (s, 3H, pzCH$_3$), 5.49 (dd, $^3J_{H-H}$ = 16.1 Hz, $^3J_{Rh-H}$ = 1.4 Hz, 1H, RhCHC<u>H</u>), 5.56 (s, 1H, pzH), 5.68 (s, 1H, pzH), 5.85 (s, 1H, pzH), 7.12 (ddd, $^3J_{H-H}$ = 16.1 Hz, $^2J_{Rh-H}$ = $^3J_{PH}$ = 2.5 Hz, 1H, RhCH). ^{31}P{^{1}H} NMR (400 MHz, C_6D_6): δ 4.27 (d, $^1J_{Rh-P}$ = 146.9 Hz).

*For Tp′Rh(PMe$_3$)(CH$_2$OC(CH$_3$)$_3$)H (**3d**).* Reaction was complete after standing overnight. The volatiles were removed to give a white solid, which was dissolved in C_6D_6. ^{1}H NMR (400 MHz, C_6D_6): δ −17.73 (dd, $^1J_{Rh-H}$ = 25.6 Hz, $^2J_{P-H}$ = 30.8 Hz, 1H, RhH), 1.26 (s, 9H, *t*Bu), 1.37 (d, $^2J_{P-H}$ = 9.5 Hz, 9H, PMe$_3$), 2.17 (s, 3H, pzCH$_3$), 2.21 (s, 3H, pzCH$_3$), 2.26 (s, 3H, pzCH$_3$), 2.34 (s, 3H, pzCH$_3$), 2.49 (s, 3H, pzCH$_3$), 2.65 (s, 3H, pzCH$_3$), 4.72 (dd, $^2J_{Rh-H}$ = 4.3 Hz, $^3J_{P-H}$ = 8.1 Hz, 1H, RhCH$_2$), 4.83 (t, $^2J_{Rh-H}$ = $^3J_{P-H}$ = 3.3 Hz, 1H, RhCH$_2$), 5.60 (s, 1H, pzH), 5.66 (s, 1H, pzH), 5.83 (s, 1H, pzH). ^{31}P{^{1}H} NMR (400 MHz, C_6D_6): δ 5.34 (d, $^1J_{Rh-P}$ = 156.6 Hz).

*For Tp′Rh(PMe$_3$)(CH$_2$C≡CCH$_3$)H (**3e**).* Reaction was complete after standing overnight. The volatiles were removed to give a white solid, which was dissolved in C_6D_6. ^{1}H NMR (400 MHz, C_6D_6): δ −18.17 (dd, $^1J_{Rh-H}$ = 21.8 Hz, $^2J_{P-H}$ = 29.5 Hz, 1H, RhH), 1.42 (d, $^2J_{P-H}$ = 9.3 Hz, 9H, PMe$_3$), 1.76 (br, 3H, CH$_3$), 2.15 (s, 3H, pzCH$_3$), 2.17 (s, 3H, pzCH$_3$), 2.21 (s, 3H, pzCH$_3$), 2.28 (s, 3H, pzCH$_3$), 2.29 (s, 3H, pzCH$_3$), 2.78 (s, 3H, pzCH$_3$), 5.60 (s, 1H, pzH), 5.63 (s, 1H, pzH), 5.74 (s, 1H, pzH), the signals for Rh-CH$_2$ are overlapping with pzCH$_3$ based on the coupling in ^{1}H−^{13}C{^{1}H} HSQC NMR. ^{31}P{^{1}H} NMR (400 MHz, C_6D_6): δ 4.45 (d, $^1J_{Rh-P}$ = 149.3 Hz).

*For Tp′Rh(PMe$_3$)(CH$_2$C(═O)CH$_3$)H (**3f**).* Reaction was complete after standing overnight. The volatiles were removed to give a white solid, which was dissolved in C_6D_6. ^{1}H NMR (400 MHz, C_6D_6): δ −17.86 (dd, $^1J_{Rh-H}$ = 20.7 Hz, $^2J_{P-H}$ = 29.0 Hz, 1H, RhH), 1.21 (d, $^2J_{P-H}$ = 9.9 Hz, 9H, PMe$_3$), 2.11 (s, 6H, 2 × CH$_3$), 2.20 (s, 3H, pzCH$_3$), 2.29 (s, 3H, pzCH$_3$), 2.32 (s, 3H, pzCH$_3$), 2.49 (s, 3H, pzCH$_3$), 2.54 (s, 3H, pzCH$_3$), 3.06 (m, 2H, RhCH$_2$), 5.52 (s, 1H,

dx.doi.org/10.1021/ja4080985 | J. Am. Chem. Soc. 2013, 135, 16198−16212

pzH), 5.57 (s, 1H, pzH), 5.77 (s, 1H, pzH). $^{31}P\{^1H\}$ NMR (400 MHz, C_6D_6): δ 4.56 (d, $^1J_{Rh-P}$ = 139.3 Hz).

*For Tp′Rh(PMe$_3$)(n-pentyl)H (**3g**).* Reaction was complete after 2 h. The volatiles were removed to give white solids, which were dissolved in C_6D_6 and kept frozen prior to taking NMR spectra at 6 °C. ^1H NMR (400 MHz, C_6D_6): δ −18.46 (dd, $^1J_{Rh-H}$ = 24.9 Hz, $^2J_{P-H}$ = 32.7 Hz, 1H, RhH), 1.18 (d, $^2J_{P-H}$ = 8.8 Hz, 9H, PMe_3), 2.15 (s, 3H, $pzCH_3$), 2.18 (s, 3H, $pzCH_3$), 2.24 (s, 3H, $pzCH_3$), 2.32 (s, 3H, $pzCH_3$), 2.38 (s, 3H, $pzCH_3$), 2.58 (s, 3H, $pzCH_3$), 5.63 (s, 1H, pzH), 5.68 (s, 1H, pzH), 5.83 (s, 1H, pzH); the signals for $RhCH_2$ and pentyl are indistinguishable due to overlapping with $pzCH_3$ peak or multiple couplings. $^{31}P\{^1H\}$ NMR (400 MHz, C_6D_6): δ 4.49 (d, $^1J_{Rh-P}$ = 155.1 Hz).

*For Tp′Rh(PMe$_3$)(c-pentyl)H (**3h**).* Exchange reaction of **2** in cyclopentane underwent decomposition rapidly at room temperature. Photolysis of 5 mg (0.010 mmol) of **1** in 0.5 mL of cyclopentane at 10 °C for 10 min led to formation of **3h** (~50%) with a trace amount of bisphosphine complex. The volatiles were removed, and the pale-yellow residue was dissolved in 0.3 mL of THF-d_8 and 0.3 mL of C_6D_6. NMR spectra were taken at −20 °C. ^1H NMR (400 MHz, C_6D_6): δ −18.75 (dd, $^1J_{Rh-H}$ = 24.5 Hz, $^2J_{P-H}$ = 32.2 Hz, 1H, RhH), 1.20 (d, $^2J_{P-H}$ = 9.0 Hz, 9H, PMe_3), 2.06 (s, 3H, $pzCH_3$), 2.09 (s, 3H, $pzCH_3$), 2.14 (s, 3H, $pzCH_3$), 2.19 (s, 3H, $pzCH_3$), 2.28 (s, 6H, 2 × $pzCH_3$), 5.53 (s, 1H, pzH), 5.54 (s, 1H, pzH), 5.74 (s, 1H, pzH); signals for RhCH and *c*-pentyl are indistinguishable due to overlapping with $pzCH_3$ peak or multiple couplings. $^{31}P\{^1H\}$ NMR (400 MHz, C_6D_6): δ 4.75 (d, $^1J_{Rh-P}$ = 155.0 Hz).

*For Tp′Rh(PMe$_3$)(CH$_2$CF$_3$)H (**3i**).* Reaction was complete after 1 d. The volatiles were removed to give a white solid, which was dissolved in C_6D_6. ^1H NMR (400 MHz, C_6D_6): δ −17.58 (dd, $^1J_{Rh-H}$ = 23.3 Hz, $^2J_{PH}$ = 30.0 Hz, RhH), 1.11 (d, $^2J_{P-H}$ = 9.7 Hz, 9H, PMe_3), 2.07 (s, 3H, $pzCH_3$), 2.12 (s, 3H, $pzCH_3$), 2.22 (s, 3H, $pzCH_3$), 2.24 (s, 3H, $pzCH_3$), 2.32 (s, 3H, $pzCH_3$), 2.54 (s, 3H, $pzCH_3$), 5.47 (s, 1H, pzH), 5.58 (s, 1H, pzH), 5.72 (s, 1H, pzH); signals for $RhCH_2$ are presumably overlapping with those for $pzCH_3$. ^{19}F NMR (400 MHz, C_6D_{12}): δ 13.65 (dt, $^3J_{H-F}$ = 15.8 Hz, $^3J_{Rh-F}$ = 5.8 Hz). $^{31}P\{^1H\}$ NMR (400 MHz, C_6D_6): δ 5.48 (d, $^1J_{Rh-P}$ = 137.8 Hz).

*For Tp′Rh(PMe$_3$)(CH$_2$F)H (**3j**).* Reaction was complete after 2 weeks. The volatiles were removed to give a white solid, which was dissolved in C_6D_6. ^1H NMR (400 MHz, C_6D_6): δ −17.49 (ddd, $^3J_{F-H}$ = 15.0 Hz, $^1J_{Rh-H}$ = 25.3 Hz, $^2J_{P-H}$ = 31.2 Hz, 1 H, RhH), 1.31 (d, $^2J_{P-H}$ = 9.4 Hz, 9H, PMe_3), 2.14 (s, 6H, 2 × $pzCH_3$), 2.22 (s, 3H, $pzCH_3$), 2.28 (s, 3H, $pzCH_3$), 2.30 (s, 3H, $pzCH_3$), 2.66 (s, 3H, $pzCH_3$), 5.58 (s, 1H, pzH), 5.64 (s, 1H, pzH), 5.74 (s, 1H, pzH), 6.49 (d of quintet, J = 3.6 Hz, $^2J_{F-H}$ = 50.5 Hz, 1H, RhCH), 6.57 (dt, $^2J_{Rh-H}$ = $^3J_{P-H}$ = 3.9 Hz, $^2J_{F-H}$ = 50.3 Hz, 1H, RhCH). ^{19}F NMR (400 MHz, C_6D_{12}): δ −143.49 (dddt, $^2J_{CH2-F}$ = 51.2 Hz, $^3J_{RhH-F}$ = 15.2 Hz, $^2J_{Rh-F}$ = 6.6 Hz, $^3J_{P-F}$ = 18.7 Hz, 3F). $^{31}P\{^1H\}$ NMR (400 MHz, C_6D_6): δ 5.13 (dd, $^3J_{F-P}$ = 19.0 Hz, $^1J_{Rh-P}$ = 151.0 Hz). Because an impurity of dimethyl ether was detected (NMR and GC-MS) as high as 16% in the gas tank, the side product was successfully assigned as Tp′Rh(PMe_3)-(CH_2OCH_3)H (**3k**).

*For Tp′Rh(PMe$_3$)(CH$_2$OCH$_3$)H (**3k**).* Reaction of crude **2** (without flash chromatography) with fluoromethane after 2 weeks gave a major product assigned as (**3k**) (73%), together with an unknown product (27%) (with zirconium salts present, no **3j** is observed.) ^1H NMR (400 MHz, C_6D_6): δ −17.87 (dd, $^1J_{Rh-H}$ = 24.8 Hz, $^2J_{P-H}$ = 31.4 Hz, 1 H, RhH), 1.34 (d, $^2J_{P-H}$ = 9.4 Hz, 9H, PMe_3), 2.18 (s, 6H, 2 × $pzCH_3$), 2.24 (s, 3H, $pzCH_3$), 2.31 (s, 3H, $pzCH_3$), 2.40 (s, 3H, $pzCH_3$), 2.66 (s, 3H, $pzCH_3$), 3.33 (s, 3H, OCH_3), 4.75 (m, 2H, $RhCH_2$), 5.65 (s, 1H, pzH), 5.66 (s, 1H, pzH), 5.79 (s, 1H, pzH). $^{31}P\{^1H\}$ NMR (400 MHz, C_6D_6): δ 5.38 (d, $^1J_{RhP}$ = 153.9 Hz).

*For Tp′Rh(PMe$_3$)(CHF$_2$)H (**3l**).* Reaction was complete after 1 week. The mixture was filtered to give a clear colorless solution, and an NMR spectrum was taken in C_6D_{12}. ^1H NMR (500 MHz, C_6D_{12}): δ −17.52 (ddt, $^3J_{F-H}$ = 17.8 Hz, $^3J_{H-H}$ = 2.6 Hz, $^1J_{Rh-H}$ = $^2J_{P-H}$ = 26.5 Hz, 1 H, RhH), 1.58 (dd, $^5J_{F-H}$ = 0.7 Hz, $^2J_{P-H}$ = 9.7 Hz, 9H, PMe_3), 2.20 (s, 3H, $pzCH_3$), 2.29 (s, 3H, $pzCH_3$), 2.29 (s, 6H, 2 × $pzCH_3$), 2.34 (s, 3H, $pzCH_3$), 2.40 (s, 3H, $pzCH_3$), 5.56 (s, 1H, pzH), 5.63 (s, 1H, pzH), 5.69 (s, 1H, pzH), 7.29 (tt, 1H, $^2J_{Rh-H}$ = $^3J_{H-H}$ = 2.6 Hz, $^2J_{F-H}$ = 55.6 Hz, 1H, RhCH). $^{13}C\{^1H\}$ NMR (500 MHz, C_6D_{12}): δ 13.62 (s, $pzCH_3$), 13.94 (s, $pzCH_3$), 14.11 (s, $pzCH_3$), 15.69 (s, $pzCH_3$), 16.62 (d, $^5J_{F-C}$ = 12.4 Hz, $pzCH_3$), 17.54 (s, $pzCH_3$), 21.89 (d, $^1J_{P-C}$ = 31.5 Hz, $P(CH_3)_3$), 107.27 (s, pzCH), 107.39 (d, $^4J_{P-C}$ = 3.2 Hz, pzCH), 108.45 (s, pzCH), 144.18 (d, $^4J_{P-C}$ = 2.1 Hz, pzCq), 144.51 (s, pzCq), 145.11 (s, pzCq), 150.03 (s, pzCq), 150.57 (d, $^3J_{P-C}$ = 2.9 Hz, pzCq), 152.07 (s, pzCq); signals for $RhCHF_2$ are invisible due to multicoupling but were able to be localized at 133.91 ppm with a general triplet splitting pattern ($^1J_{F-C}$ = 283 Hz) via the $^1H-^{13}C\{^1H\}$ HSQC coupling. ^{19}F NMR (400 MHz, C_6D_{12}): δ −16.08 (dddd, $^2J_{Rh-F}$ = 7.3 Hz, $^3J_{P-F}$ = 14.6 Hz, $^2J_{CH-F}$ = 56.4 Hz, $^2J_{F-F}$ = 243.7 Hz, 1 F), −9.60 (ddddd, $^2J_{Rh-F}$ = 9.1 Hz, $^3J_{RhH-F}$ = 17.8 Hz, $^3J_{P-F}$ = 28.5 Hz, $^2J_{CH-F}$ = 54.1 Hz, $^2J_{F-F}$ = 243.7 Hz, 1 F). $^{31}P\{^1H\}$ NMR (C_6D_{12}): δ 5.98 (ddd, $^3J_{F-P}$ = 14.6 Hz, $^3J_{F-P}$ = 28.5 Hz, $^1J_{Rh-P}$ = 153.2 Hz).

Preparation of Tp′Rh(PMe$_3$)(R)Br (4b−g): General Procedure. To the resulting solution of **3b−g** (0.019 mmol, ~10 mg) in the corresponding solvent of RH, 7.3 μL of $CHBr_3$ (0.083 mmol) was added. The mixture was stirred at room temperature overnight (1 h for **3b** and **3g**), then the crude product was purified by chromatography with 5:1 hexane−THF as the eluent (for **4f**, 6:1 hexane−ethyl acetate was used). One major side product was able to be assigned as Tp′Rh(PMe_3)Br_2 (**8**).

*For Tp′Rh(PMe$_3$)(CH$_2$C$_6$H$_3$-3,5-(CH$_3$)$_2$)Br (**4b**).* Yield: 3.9 mg (30%). ^1H NMR (500 MHz, C_6D_6): δ 1.13 (d, $^2J_{PH}$ = 10.1 Hz, 9H, PMe_3), 1.83 (s, 3H, $pzCH_3$), 2.09 (s, 6H, 2 × $arylCH_3$), 2.19 (s, 3H, $pzCH_3$), 2.25 (s, 3H, $pzCH_3$), 2.28 (s, 3H, $pzCH_3$), 2.67 (s, 3H, $pzCH_3$), 2.73 (s, 3H, $pzCH_3$), 4.67 (m, 1H, $RhCH_2$), 5.01 (d, $^2J_{H-H}$ = 12.1 Hz, 1H, $RhCH_2$), 5.41 (s, 1H, pzH), 5.50 (s, 1H, pzH), 5.69 (s, 1H, pzH), 6.66 (s, 2H, 2 × arylH), 7.16 (s, 1H, arylH, overlapping with C_6D_6). $^{13}C\{^1H\}$ NMR (500 MHz, C_6D_6): δ 12.86 (s, $pzCH_3$), 13.04 (s, $pzCH_3$), 13.40 (s, $pzCH_3$), 15.52 (s, $pzCH_3$), 17.56 (dd, $^1J_{Rh-C}$ = 8.0 Hz, $^2J_{P-C}$ = 21.2 Hz, $RhCH_2$), 16.79 (s, $pzCH_3$), 16.92 (s, $pzCH_3$), 16.92 (d, $^1J_{P-C}$ = 33.5 Hz, $P(CH_3)_3$), 21.39 (s, 2 × $arylCH_3$), 109.41 (d, $^4J_{P-C}$ = 4.2 Hz, pzCH), 108.58 (s, pzCH), 108.77 (s, pzCH), 125.68 (s, $arylCH_3$), 136.00 (s, 2 × arylCq), 142.72 (d, $^4J_{P-C}$ = 2.4 Hz, pzCq), 143.91 (s, pzCq), 144.84 (s, pzCq), 149.79 (s, arylCq), 152.78 (s, pzCq), 153.00 (s, pzCq), 153.94 (d, $^3J_{P-C}$ = 4.1 Hz, pzCq). The other aryl CH peak (s, 2C's) is overlapping with C_6D_6, which has δ = 128.34 in THF-d_8. $^{31}P\{^1H\}$ NMR (400 MHz, C_6D_6): δ −2.28 (d, $^1J_{Rh-P}$ = 127.7 Hz).

*For Tp′Rh(PMe$_3$)(CH═CHC(CH$_3$)$_3$)Br (**4c**).* Yield: 4.8 mg (40%). ^1H NMR (400 MHz, C_6D_6): δ 1.17 (s, 9H, *t*Bu), 1.19 (d, $^2J_{P-H}$ = 10.4 Hz, 9H, PMe_3), 2.11 (s, 3H, $pzCH_3$), 2.14 (s, 3H, $pzCH_3$), 2.16 (s, 3H, $pzCH_3$), 2.28 (s, 3H, $pzCH_3$), 2.74 (s, 3H, $pzCH_3$), 2.84 (s, 3H, $pzCH_3$), 5.40 (d, $^3J_{H-H}$ = 14.8 Hz, 1H, RhCHC<u>H</u>), 5.55 (s, 1H, pzH), 5.60 (s, 1H, pzH), 5.70 (s, 1H, pzH), 7.26 (dt, $^3J_{H-H}$ = 14.8 Hz, $^2J_{Rh-H}$ = $^3J_{P-H}$ = 3.2 Hz, 1H, RhCH). $^{13}C\{^1H\}$ NMR (400 MHz, C_6D_6): δ12.78 (s, $pzCH_3$), 12.94 (s, $pzCH_3$), 13.40 (s, $pzCH_3$), 16.65 (s, $pzCH_3$), 16.89 (s, $pzCH_3$), 17.33 (s, $pzCH_3$), 16.93 (d, $^1J_{P-C}$ = 34.1 Hz, $P(CH_3)_3$), 30.27 (s, $C(\underline{C}H_3)_3$), 35.62 (s, $\underline{C}(CH_3)_3$), 108.04 (d, $^4J_{P-C}$ = 4.7 Hz, pzCH), 108.40 (s, pzCH), 108.86 (s, pzCH), 142.57 (d, $^4J_{P-C}$ = 3.0 Hz, pzCq), 143.78 (s, pzCq), 144.80 (s, pzCq), 146.09 (d, $^2J_{Rh-C}$ = 1.5 Hz, RhCH<u>C</u>H), 151.49 (s, pzCq), 153.08 (d, $^3J_{P-C}$ = 5.9 Hz, pzCq), 153.11 (s, pzCq). The RhCH peak is missing due to multiple coupling with rhodium and phosphine. $^{31}P\{^1H\}$ NMR (400 MHz, C_6D_6): δ − 1.68 (d, $^1J_{Rh-P}$ = 126.1 Hz). Anal. Calcd for $C_{24}H_{42}BBrN_6PRh$: C, 45.10; H, 6.62; N, 13.15. Found: C, 45.36; H, 6.63; N, 13.81.

*For Tp′Rh(PMe$_3$)(CH$_2$OC(CH$_3$)$_3$)Br (**4d**).* Yield: 12.2 mg (99%). ^1H NMR (400 MHz, C_6D_6): δ 1.24 (d, $^2J_{P-H}$ = 10.8 Hz, 9H, PMe_3), 1.35 (s, 9H, *t*Bu), 2.10 (s, 3H, $pzCH_3$), 2.23 (s, 3H, $pzCH_3$), 2.33 (s, 3H, $pzCH_3$), 2.44 (s, 3H, $pzCH_3$), 2.71 (s, 3H, $pzCH_3$), 2.90 (s, 3H, $pzCH_3$), 5.21 (d, $^2J_{Rh-H}$ = 3.6 Hz, 1H, $RhCH_2$), 5.40 (s, 1H, pzH), 5.63 (s, 1H, pzH), 5.71 (s, 1H, pzH), 6.77 (d, $^2J_{Rh-H}$ = 3.2 Hz, 1H, $RhCH_2$). $^{13}C\{^1H\}$ NMR (500 MHz, C_6D_6): δ 12.77 (s, $pzCH_3$), 12.99 (s, $pzCH_3$), 13.53 (s, $pzCH_3$), 14.61 (s, $pzCH_3$), 15.59 (s, $pzCH_3$), 17.21 (s, $pzCH_3$), 17.71 (d, $^1J_{PC}$ = 33.5 Hz, $P(CH_3)_3$), 28.32 (s, $C(\underline{C}H_3)_3$), 52.80 (dd, $^1J_{Rh-C}$ = 5.0 Hz, $^2J_{P-C}$ = 21.0 Hz, $RhCH_2$),

dx.doi.org/10.1021/ja4080985 | J. Am. Chem. Soc. 2013, 135, 16198−16212

74.45 (s, $\underline{C}(CH_3)_3$), 108.06 (s, pzCH), 108.45 (d, $^4J_{P-C}$ = 3.9 Hz, pzCH), 109.10 (s, pzCH), 142.75 (d, $^4J_{P-C}$ = 2.3 Hz, pzCq), 142.87 (s, pzCq), 146.07 (s, pzCq), 152.03 (s, pzCq), 152.14 (d, $^3J_{P-C}$ = 4.6 Hz, pzCq), 153.57 (s, pzCq). $^{31}P\{^1H\}$ NMR (400 MHz, C_6D_6): δ 0.19 (d, $^1J_{Rh-P}$ = 138.5 Hz). Anal. Calcd for $C_{23}H_{42}BBrN_6OPRh$: C, 42.95; H, 6.58; N, 13.07. Found: C, 43.20; H, 6.58; N, 12.87.

*For Tp′Rh(PMe$_3$)(CH$_2$C≡CCH$_3$)Br (**4e**).* Yield: 5.9 mg (52%). ^1H NMR (400 MHz, C_6D_6): δ 1.13 (d, $^2J_{P-H}$ = 10.4 Hz, 9H, PMe_3), 1.24 (br, 3H, CH_3), 2.12 (s, 3H, pzCH$_3$), 2.18 (s, 3H, pzCH$_3$), 2.28 (s, 3H, pzCH$_3$), 2.29 (s, 3H, pzCH$_3$), 2.71 (s, 3H, pzCH$_3$), 3.08 (s, 3H, pzCH$_3$), 3.38 (m, 1H, RhCH$_2$), 4.35 (td, $^2J_{H-H}$ = 13.6 Hz, $^2J_{Rh-H}$ = $^3J_{P-H}$ = 2.8 Hz, 1H, RhCH$_2$), 5.54 (s, 1H, pzH), 5.64 (s, 1H, pzH), 5.68 (s, 1H, pzH). $^{13}C\{^1H\}$ NMR (500 MHz, C_6D_6): δ − 4.07 (dd, $^1J_{Rh-C}$ = 7.6 Hz, $^2J_{P-C}$ = 20.1 Hz, RhCH$_2$), 4.63 (s, CH_3), 12.95 (s, pzCH$_3$), 12.98 (s, pzCH$_3$), 13.40 (s, pzCH$_3$), 15.32 (s, pzCH$_3$), 16.34 (s, pzCH$_3$), 16.55 (d, $^1J_{P-C}$ = 33.5 Hz, P(CH$_3$)$_3$), 17.13 (s, pzCH$_3$), 75.33 (s, RhCH$_2$C≡$\underline{C}$), 89.88 (s, RhCH$_2$$\underline{C}$≡C), 107.98 (d, $^4J_{P-C}$ = 4.4 Hz, pzCH), 108.70 (s, pzCH), 108.90 (s, pzCH), 142.28 (d, $^4J_{P-C}$ = 2.3 Hz, pzCq), 144.09 (s, pzCq), 144.43 (s, pzCq), 152.39 (s, pzCq), 154.00 (s, pzCq), 153.36 (d, $^3J_{P-C}$ = 4.7 Hz, pzCq). $^{31}P\{^1H\}$ NMR (400 MHz, C_6D_6): δ − 0.87 (d, $^1J_{Rh-P}$ = 125.0 Hz).

*For Tp′Rh(PMe$_3$)(CH$_2$C(=O)CH$_3$)Br (**4f**).* Yield: 3.8 mg (33%). ^1H NMR (500 MHz, C_6D_6): δ 1.28 (d, $^2J_{P-H}$ = 10.8 Hz, 9H, PMe_3), 2.09 (s, 3H, pzCH$_3$), 2.13 (s, 3H, pzCH$_3$), 2.22 (s, 3H, pzCH$_3$), 2.38 (s, 3H, pzCH$_3$), 2.38 (s, 3H, CH_3), 2.63 (s, 3H, pzCH$_3$), 2.99 (s, 3H, pzCH$_3$), 4.00 (d, $^2J_{H-H}$ = 8.9 Hz, 1H, RhCH$_2$), 4.27 (d, $^2J_{H-H}$ = 8.6 Hz, 1H, RhCH$_2$), 5.50 (s, 2H, 2 × pzH), 5.59 (s, 1H, pzH). $^{13}C\{^1H\}$ NMR (500 MHz, C_6D_6): δ12.77 (s, pzCH$_3$), 12.87 (s, pzCH$_3$), 13.41 (s, pzCH$_3$), 15.76 (s, pzCH$_3$), 16.42 (dd, $^1J_{Rh-C}$ = 7.6 Hz, $^2J_{P-C}$ = 21.4 Hz, RhCH$_2$), 17.25 (s, pzCH$_3$), 17.58 (s, pzCH$_3$), 17.88 (d, $^1J_{P-C}$ = 33.9 Hz, P(CH$_3$)$_3$), 33.93 (s, CH_3), 108.72 (s, pzCH), 108.98 (d, $^4J_{P-C}$ = 4.1 Hz, pzCH), 110.05 (s, pzCH), 143.03 (d, $^4J_{P-C}$ = 2.6 Hz, pzCq), 143.30 (s, pzCq), 145.76 (s, pzCq), 152.84 (s, pzCq), 152.86 (d, $^3J_{P-C}$ = 4.4 Hz, pzCq), 153.44(s, pzCq), 220.12 (s, C(=O)). $^{31}P\{^1H\}$ NMR (500 MHz, C_6D_6): δ − 2.02 (d, $^1J_{Rh-P}$ = 123.9 Hz). Anal. Calcd for $C_{21}H_{36}BBrN_6OPRh$: C, 41.14; H, 5.92; N, 13.71. Found: C, 41.03; H, 5.87; N, 13.59.

*For Tp′Rh(PMe$_3$)(n-pentyl)Br (**4g**).* Yield: 6.2 mg (52%). ^1H NMR (400 MHz, C_6D_6): δ 0.84 (t, $^3J_{H-H}$ = 7.3 Hz, 3H, pentyl), 1.17 (d, $^2J_{P-H}$ = 10.1 Hz, 9H, PMe_3), 1.27 (m, 2H, pentyl), 1.48 (m, 2H, pentyl), 1.58 (m, 2H, pentyl), 2.09 (s, 3H, pzCH$_3$), 2.09 (s, 3H, pzCH$_3$), 2.15 (s, 3H, pzCH$_3$), 2.27 (s, 3H, pzCH$_3$), 2.68 (m, 1H, RhCH$_2$), 2.71 (s, 3H, pzCH$_3$), 2.93 (s, 3H, pzCH$_3$), 4.24 (m, 1H, RhCH$_2$), 5.56 (s, 1H, pzH), 5.64 (s, 1H, pzH), 5.69 (s, 1H, pzH). $^{13}C\{^1H\}$ NMR (500 MHz, C_6D_6): δ 12.96 (s, 2 × pzCH$_3$), 13.50 (s, pzCH$_3$), 14.64 (s, pentyl-CH$_3$), 15.77 (s, pzCH$_3$), 15.87 (s, pzCH$_3$), 16.85 (s, pzCH$_3$), 16.85 (d, $^1J_{P-C}$ = 33.5 Hz, P(CH$_3$)$_3$), 18.10 (dd, $^1J_{Rh-C}$ = 7.4 Hz, $^2J_{P-C}$ = 20.3 Hz, RhCH$_2$), 23.11 (s, pentyl-CH$_2$), 32.96 (s, pentyl-CH$_2$), 35.09 (s, pentyl-CH$_2$), 108.11 (d, $^4J_{P-C}$ = 4.1 Hz, pzCH), 108.38 (s, pzCH), 108.86 (s, pzCH), 142.86 (d, $^4J_{P-C}$ = 2.4 Hz, pzCq), 143.98 (s, pzCq), 144.56 (s, pzCq), 151.46 (s, pzCq), 153.02 (d, $^3J_{P-C}$ = 4.3 Hz, pzCq), 153.32 (s, pzCq). $^{31}P\{^1H\}$ NMR (400 MHz, C_6D_6): δ − 2.30 (d, $^1J_{Rh-P}$ = 128.6 Hz).

*For Tp′Rh(PMe$_3$)(n-pentyl)Cl (**4g**-Cl).* Pentylmagnesiumchloride (0.100 mL of a 2 M solution in THF, 0.200 mmol) was added dropwise to 100 mg (0.183 mmol) of Tp′Rh(PMe$_3$)Cl$_2$ in 15 mL of THF. The reaction mixture was stirred for 20 min. The color of the solution changed from orange to yellow upon addition of the Grignard reagent. The reaction was quenched with 1.5 mL of saturated NH_4Cl(aq) solution. The volatiles were evaporated under vacuum, and 5 mL of methylene chloride was then added to give a cloudy mixture. This mixture was filtered through Celite and layered with hexanes for recrystallization. Light orange-yellow crystals were collected (94.5 mg, 89%) and dissolved in C_6D_6. ^1H NMR (400 MHz, C_6D_6): δ 0.85 (t, $^3J_{H-H}$ = 7.3 Hz, 3H, pentyl), 1.11 (d, $^2J_{P-H}$ = 10.1 Hz, 9H, PMe_3), 1.30 (sextet, $^3J_{H-H}$ =6.9 Hz, 2H, pentyl), 1.53 (m, 2H, pentyl), 1.60 (m, 2H, pentyl), 2.09 (s, 6H, 2 × pzCH$_3$), 2.17 (s, 3H, pzCH$_3$), 2.27 (s, 3H, pzCH$_3$), 2.68 (s, 3H, pzCH$_3$), 2.74 (m, 1H, RhCH$_2$), 2.91 (s, 3H, pzCH$_3$), 4.01 (m, 1H, RhCH$_2$), 5.56 (s, 1H, pzH), 5.65 (s, 1H, pzH), 5.69 (s, 1H, pzH). $^{13}C\{^1H\}$ NMR (500 MHz, C_6D_6): δ 12.96 (s, 2 × pzCH$_3$), 13.54 (s, pzCH$_3$), 14.67 (s, 2C's, pzCH$_3$ and pentyl-CH$_3$), 15.90 (s, pzCH$_3$), 15.98 (d, $^1J_{P-C}$ = 33.0 Hz, P(CH$_3$)$_3$), 16.18 (s, pzCH$_3$), 19.28 (dd, $^1J_{Rh-C}$ = 7.3 Hz, $^2J_{P-C}$ = 20.7 Hz, RhCH$_2$), 23.11 (s, pentyl-CH$_2$), 32.77 (s, pentyl-CH$_2$), 35.12 (s, pentyl-CH$_2$), 107.97 (d, $^4J_{P-C}$ = 4.5 Hz, pzCH), 108.25 (s, pzCH), 108.78 (s, pzCH), 142.70 (d, $^4J_{P-C}$ = 2.5 Hz, pzCq), 143.96 (s, pzCq), 144.69 (s, pzCq), 151.51 (s, pzCq), 152.48 (d, $^3J_{P-C}$ = 4.3 Hz, pzCq), 152.95 (s, pzCq). $^{31}P\{^1H\}$ NMR (400 MHz, C_6D_6): δ − 0.35 (d, $^1J_{Rh-P}$ = 130.7 Hz). Anal. Calcd for $C_{23}H_{42}BClN_6PRh$: C, 47.40; H, 7.26; N, 14.42. Found: C, 47.54; H, 7.31; N, 14.29.

*For Tp′Rh(PMe$_3$)(c-pentyl)Cl (**4h**-Cl).* The synthesis of **4h**-Cl was identical to that of **4g**-Cl except that *c*-pentylmagnesiumchloride was used. The product was isolated as light orange powder by flash chromatography using 5:1 hexane−ethyl acetate as the eluent. The major side product was assigned as Tp′Rh(PMe$_3$)(Cl)H (**5**). Yield: 36.0 mg (34%). ^1H NMR (500 MHz, C_6D_6): δ 1.13 (d, $^2J_{P-H}$ = 10.1 Hz, 9H, PMe_3), 2.05 (s, 3H, pzCH$_3$), 2.12 (s, 3H, pzCH$_3$), 2.19 (s, 3H, pzCH$_3$), 2.27 (s, 3H, pzCH$_3$), 2.66 (s, 3H, pzCH$_3$), 2.86 (s, 3H, pzCH$_3$), 5.56 (s, 1H, pzH), 5.58 (s, 1H, pzH), 5.68 (s, 1H, pzH), signals for RhCH and *c*-pentyl are indistinguishable due to overlapping with pzCH$_3$ peak or multicoupling. $^{31}P\{^1H\}$ NMR (400 MHz, C_6D_6): δ 0.27 (br d, $^1J_{Rh-P}$ = 131.8 Hz). $^{31}P\{^1H\}$ NMR was also conducted at varied temperatures (25 °C, 0 °C, −30 °C, −50 °C). Anal. Calcd for $C_{23}H_{40}BClN_6PRh{\cdot}0.8C_4H_8O$: C, 49.29; H, 7.33; N, 13.16. Found: C, 49.29; H, 7.18; N, 13.50.

*For Tp′Rh(PMe$_3$)(CH$_2$CF$_3$)Br (**4i**).* Yield: 2.6 mg (21%). ^1H NMR (500 MHz, $CDCl_3$): δ 1.55 (d, $^2J_{P-H}$ = 10.4 Hz, 9H, PMe_3), 2.30 (s, 3H, pzCH$_3$), 2.38 (s, 3H, pzCH$_3$), 2.40 (s, 3H, pzCH$_3$), 2.40 (s, 3H, pzCH$_3$), 2.61 (s, 3H, pzCH$_3$), 2.66 (s, 3H, pzCH$_3$), 3.20 (t of quintet, $^2J_{Rh-H}$ = $^3J_{P-H}$ = 3.2 Hz, $^3J_{F-H}$ = $^2J_{H-H}$ = 14.5 Hz, 1H, RhCH$_2$), 3.55 (t of quintet, $^2J_{Rh-H}$ = $^3J_{P-H}$ = 2.5 Hz, $^3J_{F-H}$ = $^2J_{H-H}$ = 14.5 Hz, 1H, RhCH$_2$), 5.75 (s, 1H, pzH), 5.77 (s, 1H, pzH), 5.79 (s, 1H, pzH). $^1H\{^{31}P\}$ NMR was also taken to confirm coupling patterns for the methylene hydrogens. $^{13}C\{^1H\}$ NMR (500 MHz, $CDCl_3$): δ 4.83 (d of quintets, J_1 = 9.9 Hz, J_2 = 25.3 Hz, RhCH$_2$), 13.04 (s, pzCH$_3$), 13.13 (s, pzCH$_3$), 13.73 (s, pzCH$_3$), 15.76 (d, $^6J_{F-C}$ = 1.9 Hz, pzCH$_3$), 17.04 (s, pzCH$_3$), 17.27 (d, $^7J_{F-C}$ = 0.9 Hz, pzCH$_3$), 18.58 (d, $^1J_{P-C}$ = 34.1 Hz, P(CH$_3$)$_3$), 108.54 (d, $^4J_{P-C}$ = 4.4 Hz, pzCH), 108.83 (s, pzCH), 110.06 (s, pzCH), 133.47 (q, $^1J_{F-C}$ = 278.5 Hz, CF_3), 143.42 (d, $^4J_{P-C}$ = 2.7 Hz, pzCq), 143.73 (s, pzCq), 145.55 (s, pzCq), 152.20 (s, pzCq), 152.47 (s, pzCq), 153.09 (d, $^3J_{P-C}$ = 4.4 Hz, pzCq). ^{19}F NMR (400 MHz, C_6D_{12}): δ 16.32 (t, $^3J_{H-F}$ = 14.5 Hz). $^{31}P\{^1H\}$ NMR (400 MHz, C_6D_6): δ −1.87 (d, $^1J_{Rh-P}$ = 119.0 Hz). Anal. Calcd for $C_{20}H_{33}BBrF_3N_6PRh$: C, 37.59; H, 5.20; N, 13.15. Found: C, 37.66; H, 5.20; N, 13.07.

*For [Tp′Rh(PMe$_3$)(THF)H]$^+$ BF$_4^-$ (**6**).* ^1H NMR (400 MHz, THF-d_8): δ −15.16 (dd, $^1J_{Rh-H}$ = 12.5 Hz, $^2J_{P-H}$ = 23.6 Hz, 1H, RhH), 1.56 (d, $^2J_{P-H}$ = 10.8 Hz, 9H, PMe_3), 2.29 (s, 3H, pzCH$_3$), 2.31 (s, 3H, pzCH$_3$), 2.33 (s, 3H, pzCH$_3$), 2.35 (s, 3H, pzCH$_3$), 2.37 (s, 3H, pzCH$_3$), 2.53 (s, 3H, pzCH$_3$), 5.81 (s, 1H, pzH), 5.91 (s, 1H, pzH), 6.07 (s, 1H, pzH). $^{31}P\{^1H\}$ NMR (400 MHz, THF-d_8): δ 1.43 (d, $^1J_{Rh-P}$ = 120.9 Hz).

*For Tp′Rh(PMe$_3$)(η^2−CH$_3$C≡CCH$_3$) (**7**).* Compound **7** was synthesized by heating the solution of **3e** (~10 mg) in 0.5 mL of C_6D_6 at 30 °C for 1 week. Yield: 73% by NMR. Yellow block crystals were recrystallized by slow evaporation of diethyl ether. ^1H NMR (400 MHz, C_6D_6): δ 0.73 (d, $^2J_{P-H}$ = 9.5 Hz, 9H, PMe_3), 2.13 (s, 3H, pzCH$_3$), 2.23 (s, 3H, pzCH$_3$), 2.24 (s, 6H, 2 × CH$_3$), 2.38 (s, 6H, 2 × pzCH$_3$), 2.57 (s, 6H, 2 × pzCH$_3$), 5.32 (s, 1H, pzH), 5.89 (s, 2H, 2 × pzH). $^{11}B\{^1H\}$ NMR (500 MHz, THF-d_8): δ −8.31 (s). $^{31}P\{^1H\}$ NMR (400 MHz, C_6D_6): δ 10.66 (d, $^1J_{Rh-P}$ = 159.5 Hz). IR (cm^{-1}): 1967 (C≡C), 2543 (B−H).

*For Tp′Rh(PMe$_3$)Br$_2$ (**8**).* ^1H NMR (400 MHz, C_6D_6): δ 1.36 (d, $^2J_{PH}$ = 11.1 Hz, 9H, PMe_3), 2.10 (s, 9H, 3 × pzCH$_3$), 2.60 (s, 6H, 2 × pzCH$_3$), 3.28 (s, 3H, pzCH$_3$), 5.46 (s, 2H, 2 × pzH), 5.54 (s, 1H, pzH). $^{31}P\{^1H\}$ NMR (400 MHz, C_6D_6): δ − 0.92 (d, $^1J_{Rh-P}$ = 104.8 Hz).

dx.doi.org/10.1021/ja4080985 | J. Am. Chem. Soc. 2013, 135, 16198−16212

Preparation of Tp′Rh(PMe$_3$)(C≡CR)H (3m−s): General Procedures. (Method 1) A resealable 5 mm NMR tube containing 20 mg (0.042 mmol) of **1** was charged with 0.5 mL of HC≡CR (R = CMe$_3$, SiMe$_3$, or *n*-hexyl) under nitrogen. The sample was irradiated for 15 min to give a light yellow solution. The reaction was almost complete and quantitative as determined by ^{1}H NMR spectroscopy. An off-white powder was isolated after removal of solvent and directly used in kinetic study. (Method 2) Compound **2** (∼40 mg, 0.076 mmol) was *in situ* prepared and isolated as described before. For activation of 3,3,3-trifluoro-1-propyne, **2** was dissolved in 0.4 mL of C_6D_{12} and transferred to a high pressure NMR tube, followed by pressurization with 3,3,3-trifluoro-1-propyne at 15 psi. For other alkynes, the solids were directly dissolved in 0.4 mL of the corresponding HC≡CR and transferred to a resealable 5 mm J-Young NMR tube. After the reaction was complete, the solvent was removed under vacuum, and the resulting residue was dissolved in C_6D_6 for ^{1}H, ^{11}B{^{1}H}, ^{13}C{^{1}H}, ^{19}F, and ^{31}P{^{1}H} NMR spectroscopy.

*For Tp′Rh(PMe$_3$)(C≡CC(CH$_3$)$_3$)H (**3m**).* The exchange reaction was almost complete after 2 d at ambient temperature. Colorless crystals (41.8 mg, 99%) of **3m** were grown from 1:1 hexane/ether solution at room temperature. ^{1}H NMR (500 MHz, C_6D_6): δ −16.49 (dd, $^1J_{Rh-H}$ = 20.7 Hz, $^2J_{P-H}$ = 30.0 Hz, 1H, RhH), 1.27 (d, $^2J_{P-H}$ = 10.2 Hz, 9H, PMe$_3$), 1.46 (s, 9H, C(CH$_3$)$_3$), 2.09 (s, 3H, pzCH$_3$), 2.11 (s, 3H, pzCH$_3$), 2.26 (s, 3H, pzCH$_3$), 2.34 (s, 3H, pzCH$_3$), 2.82 (s, 3H, pzCH$_3$), 2.86 (s, 3H, pzCH$_3$), 5.44 (s, 1H, pzH), 5.64 (s, 1H, pzH), 5.78 (s, 1H, pzH). ^{13}C{^{1}H} NMR (500 MHz, C_6D_6): δ 12.67 (s, pzCH$_3$), 12.91 (s, 2 × pzCH$_3$), 15.88 (s, pzCH$_3$), 16.20 (s, pzCH$_3$), 16.74 (s, pzCH$_3$), 19.13 (d, $^1J_{P-C}$ = 34.5 Hz, P(CH$_3$)$_3$), 29.72 (s, C(CH$_3$)$_3$), 33.04 (s, C(CH$_3$)$_3$), 80.75 (ddd, $^1J_{Rh-C}$ = 28.1 Hz, $^2J_{P-C}$ = 45.5 Hz, $^2J_{H-C}$ = 4.3 Hz, Rh-C≡C), 105.81 (d, $^4J_{P-C}$ = 3.9 Hz, pzCH), 106.50 (s, pzCH), 107.19 (pzCH), 111.72 (d, $^2J_{Rh-C}$ = 10.3 Hz, Rh−C≡C), 142.60 (d, $^4J_{P-C}$ = 2.7 Hz, pzCq), 144.10 (s, pzCq), 144.63 (s, pzCq), 149.95 (s, pzCq), 151.01 (d, $^3J_{P-C}$ = 2.7 Hz, pzCq), 152.56 (s, pzCq). ^{31}P{^{1}H} NMR (400 MHz, C_6D_6): δ 5.71 (d, $^1J_{Rh-P}$ = 125.2 Hz). IR (cm^{-1}): 2162 (C≡C). Anal. Calcd for $C_{24}H_{41}BN_6PRh\cdot(Et_2O)_{0.45}$: C, 52.37; H, 7.75; N, 14.20. Found: C, 52.70; H, 7.66; N, 14.64.

*For Tp′Rh(PMe$_3$)(C≡CSiMe$_3$)H (**3n**).* The exchange reaction was almost complete after 2 days at ambient temperature. Colorless crystals (43.6 mg, 99%) of **3n** were grown from 1:1 hexane/ether solution at room temperature. ^{1}H NMR (500 MHz, C_6D_6): δ −16.12 (dd, $^1J_{Rh-H}$ = 21.0 Hz, $^2J_{P-H}$ = 29.4 Hz, 1H, RhH), 0.38 (s, 9H, Si(CH$_3$)$_3$), 1.25 (d, $^2J_{P-H}$ = 10.3 Hz, 9H, PMe$_3$), 2.07 (s, 6H, 2 × pzCH$_3$), 2.24 (s, 3H, pzCH$_3$), 2.32 (s, 3H, pzCH$_3$), 2.81 (s, 3H, pzCH$_3$), 2.83 (s, 3H, pzCH$_3$), 5.41 (s, 1H, pzH), 5.62 (s, 1H, pzH), 5.76 (s, 1H, pzH). ^{13}C{^{1}H} NMR (500 MHz, C_6D_6): δ 1.75 (s, Si(CH$_3$)$_3$) 12.65 (s, pzCH$_3$), 12.88 (s, 2 × pzCH$_3$), 15.91 (s, pzCH$_3$), 16.34 (s, pzCH$_3$), 16.71 (s, pzCH$_3$), 19.00 (d, $^1J_{P-C}$ = 34.7 Hz, P(CH$_3$)$_3$), 105.94 (d, $^4J_{P-C}$ = 3.7 Hz, pzCH), 106.59 (s, pzCH), 107.34 (pzCH), 110.32 (d, $^2J_{Rh-C}$ = 8.9 Hz, Rh−C≡C), 126.87 (dd, $^1J_{Rh-C}$ = 25.6 Hz, $^2J_{P-C}$ = 43.1 Hz, Rh-C≡C), 142.72 (d, $^4J_{P-C}$ = 2.7 Hz, pzCq), 144.18 (s, pzCq), 144.82 (s, pzCq), 150.04 (s, pzCq), 151.15 (d, $^3J_{P-C}$ = 2.5 Hz, pzCq), 152.72 (s, pzCq). ^{31}P{^{1}H} NMR (400 MHz, C_6D_6): δ 5.45 (d, $^1J_{Rh-P}$ = 123.9 Hz). IR (cm^{-1}): 2162 (C≡C). Anal. Calcd for $C_{23}H_{41}BN_6PRh$: C, 48.09; H, 7.19; N, 14.63. Found: C, 48.16; H, 7.18; N, 14.33.

*For Tp′Rh(PMe$_3$)(C≡Cn-hexyl)H (**3o**).* The exchange reaction was almost complete after 3 d at ambient temperature. Colorless crystals (41.7 mg, 93%) of **3o** were grown from 1:1 hexane/ether solution at room temperature. ^{1}H NMR (500 MHz, C_6D_6): δ −16.48 (dd, $^1J_{Rh-H}$ = 20.8 Hz, $^2J_{P-H}$ = 30.0 Hz, 1H, RhH), 0.89 (t, 3H, CH$_2$(CH$_2$)$_4$CH$_3$), 1.29 (d, $^2J_{P-H}$ = 10.2 Hz, 9H, PMe$_3$), 1.53 (m, 2H, (CH$_2$)$_4$CH$_2$CH$_3$), 1.69 (m, 2H, (CH$_2$)$_3$CH$_2$CH$_2$CH$_3$), 1.96 (dt, 4H, CH$_2$(CH$_2$)$_2$(CH$_2$)$_2$CH$_3$), 2.11 (s, 3H, pzCH$_3$), 2.11 (s, 3H, pzCH$_3$), 2.26 (s, 3H, pzCH$_3$), 2.34 (s, 3H, pzCH$_3$), 2,61 (t, 2H, CH$_2$(CH$_2$)$_4$CH$_3$), 2.83 (s, 3H, pzCH$_3$), 2.85 (s, 3H, pzCH$_3$), 5.46 (s, 1H, pzH), 5.64 (s, 1H, pzH), 5.78 (s, 1H, pzH). ^{13}C{^{1}H} NMR (500 MHz, C_6D_6): δ 12.70 (s, pzCH$_3$), 12.93 (s, 2 × pzCH$_3$), 14.35 (s, CH$_2$(CH$_2$)$_4$CH$_3$), 15.78 (s, pzCH$_3$), 16.22 (s, pzCH$_3$), 16.77 (s, pzCH$_3$), 19.35 (d, $^1J_{P-C}$ = 34.4 Hz, P(CH$_3$)$_3$), 22.65 (s, CH$_2$(CH$_2$)$_4$CH$_3$), 23.16 (s, (CH$_2$)$_4$CH$_2$CH$_3$), 29.46 (s, (CH$_2$)$_2$CH$_2$(CH$_2$)$_2$CH$_3$), 31.55 (s, CH$_2$CH$_2$(CH$_2$)$_3$CH$_3$), 32.11 (s, (CH$_2$)$_3$CH$_2$CH$_2$CH$_3$), 82.54 (ddd, $^1J_{Rh-C}$ = 28.0 Hz, $^2J_{P-C}$ = 45.4 Hz, $^2J_{H-C}$ = 4.4 Hz, Rh-C≡C), 102.64 (d, $^2J_{Rh-C}$ = 10.5 Hz, Rh−C≡C), 105.79 (d, $^4J_{P-C}$ = 3.9 Hz, pzCH), 106.50 (s, pzCH), 107.17 (s, pzCH), 142.57 (d, $^4J_{P-C}$ = 2.8 Hz, pzCq), 144.02 (s, pzCq), 144.66 (s, pzCq), 149.96 (s, pzCq), 150.96 (d, $^3J_{P-C}$ = 2.9 Hz, pzCq), 152.39 (s, pzCq). ^{31}P{^{1}H} NMR (400 MHz, C_6D_6): δ 5.93 (d, $^1J_{Rh-P}$ = 125.4 Hz). IR (cm^{-1}): 2161 (C≡C). Anal. Calcd for $C_{26}H_{45}BN_6PRh$: C, 53.26; H, 7.74; N, 14.33. Found: C, 53.49; H, 7.91; N, 14.24.

*For Tp′Rh(PMe$_3$)(C≡CC$_6$H$_4$-p-OMe)H (**3p**).* The exchange reaction was almost complete after 1 day at ambient temperature. Orange yellow crystals (36.1 mg, 78%) of **3p** were grown from 1:1 hexane/THF solution at room temperature. ^{1}H NMR (500 MHz, C_6D_6): δ −16.13 (dd, $^1J_{Rh-H}$ = 20.6 Hz, $^2J_{P-H}$ = 29.6 Hz, 1 H, RhH), 1.26 (d, $^2J_{P-H}$ = 10.2 Hz, 9H, PMe$_3$), 2.12 (s, 3H, pzCH$_3$), 2.12 (s, 3H, pzCH$_3$), 2.27 (s, 3H, pzCH$_3$), 2.35 (s, 3H, pzCH$_3$), 2.82 (s, 3H, pzCH$_3$), 2.88 (s, 3H, pzCH$_3$), 3.30 (s, 3H, OCH$_3$), 5.43 (s, 1H, pzH), 5.58 (s, 1H, pzH), 5.76 (s, 1H, pzH), 6.80 (d, *J* = 8.6 Hz, 2H, *p*-OMePh-*m*), 7.55 (d, *J* = 8.6 Hz, 2H, *p*-OMePh-*o*). ^{13}C{^{1}H} NMR (500 MHz, C_6D_6): δ 12.68 (s, pzCH$_3$), 12.91 (s, pzCH$_3$), 12.94 (s, pzCH$_3$), 15.69 (s, pzCH$_3$), 16.14 (s, pzCH$_3$), 16.80 (s, pzCH$_3$), 19.19 (d, $^1J_{P-C}$ = 34.5 Hz, P(CH$_3$)$_3$), 54,74 (s, OCH$_3$), 99.64 (dd, $^1J_{Rh-C}$ = 25.3 Hz, $^2J_{P-C}$ = 46.6 Hz, Rh-C≡C), 105.56 (d, $^2J_{Rh-C}$ = 10.8 Hz, Rh−C≡C), 105.94 (d, $^4J_{P-C}$ = 3.6 Hz, pzCH), 106.65 (s, pzCH), 107.33 (s, pzCH), 114.05 (s, 2C, *p*-OMePh-*m*), 123.21 (s, *p*-OMePh-*ipso*), 132.13 (s, 2C, *p*-OMePh-*o*), 142.75 (d, $^4J_{P-C}$ = 2.7 Hz, pzCq), 144.18 (s, pzCq), 144.87 (s, pzCq), 150.10 (s, pzCq), 151.06 (d, $^3J_{P-C}$ = 2.5 Hz, pzCq), 152.50 (s, pzCq), 157.50 (s, COMe). ^{31}P{^{1}H} NMR (400 MHz, C_6D_6): δ 5.55 (d, $^1J_{Rh-P}$ = 123.4 Hz). IR (cm^{-1}): 2161 (C≡C).

*For Tp′Rh(PMe$_3$)(C≡CCF$_3$)H (**3q**).* The colorless solution became light yellow after overnight. A mixture of **3q** (15%) and Tp′Rh(PMe$_3$)(η^2-HC≡CCF$_3$) (**3q**-η^2) (85%) was found based on ^{1}H and ^{31}P{^{1}H} NMR spectroscopy. Heating at 140 °C for 5 h in C_6D_6 resulted in the almost quantitative formation of **3q**. Colorless crystals (38.5 mg, 89%) of **3q** were grown from 1:1 hexane/ether solution at room temperature. ^{1}H NMR (500 MHz, C_6D_6): δ −15.74 (dd, $^1J_{Rh-H}$ = 20.0 Hz, $^2J_{P-H}$ = 28.5 Hz, 1H, RhH), 1.08 (d, $^2J_{P-H}$ = 10.4 Hz, 9H, PMe$_3$), 1.99 (s, 3H, pzCH$_3$), 2.04 (s, 3H, pzCH$_3$), 2.20 (s, 3H, pzCH$_3$), 2.29 (s, 3H, pzCH$_3$), 2.62 (s, 3H, pzCH$_3$), 2.68 (s, 3H, pzCH$_3$), 5.35 (s, 1H, pzH), 5.58 (s, 1H, pzH), 5.68 (s, 1H, pzH). ^{13}C{^{1}H} NMR (500 MHz, C_6D_6): δ 12.58 (s, pzCH$_3$), 12.80 (s, pzCH$_3$), 12.84 (s, pzCH$_3$), 15.64 (s, pzCH$_3$), 15.89 (s, pzCH$_3$), 16.70 (s, pzCH$_3$), 18.53 (d, $^1J_{P-C}$ = 34.8 Hz, P(CH$_3$)$_3$), 92.88 (dd, $^1J_{Rh-C}$ = 11.1 Hz, $^2J_{P-C}$ = 46.9 Hz, Rh-C≡C), 106.14 (d, $^4J_{P-C}$ = 3.7 Hz, pzCH), 106.84 (s, pzCH), 107.55 (s, pzCH), 143.11 (d, $^4J_{P-C}$ = 2.6 Hz, pzCq), 144.47 (s, pzCq), 145.27 (s, pzCq), 140.30 (s, pzCq), 151.14 (d, $^3J_{P-C}$ = 2.7 Hz, pzCq), 152.66 (s, pzCq); the signals for CF$_3$ and Rh−C≡C are indistinguishable due to multiple coupling with fluorines. ^{19}F NMR (400 MHz, C_6D_{12}): δ 18.81 (s, 3F). ^{31}P{^{1}H} NMR (400 MHz, C_6D_6): δ 4.79 (d, $^1J_{Rh-P}$ = 118.2 Hz). IR (cm^{-1}): 2129 (C≡C). Anal. Calcd for $C_{21}H_{32}BF_3N_6PRh$: C, 44.23; H, 5.66; N, 14.74. Found: C, 44.21; H, 5.69; N, 14.46.

Tp′Rh(PMe$_3$)(η^2-HC≡CCF$_3$) (3q-η^2). The same procedure was followed as Method 2. After 1 d, the mixture turned light yellow and a white solid formed in the NMR tube. The white powder was collected by filtration and confirmed to be **3q**-η^2 by NMR spectroscopy. The light yellow clear solution was taken in vacuo and plate X-ray quality crystals (31.5 mg, 73%) of **3q**-η^2 were grown in ether at −20 °C. ^{1}H NMR (400 MHz, C_6D_6): δ 0.62 (d, $^2J_{P-H}$ = 10.3 Hz, 9H, PMe$_3$), 2.04 (s, 3H, pzCH$_3$), 2.18 (s, 3H, pzCH$_3$), 2.33 (s, 3H, pzCH$_3$), 2.35 (s, 6H, 2 × pzCH$_3$), 2.66 (s, 3H, pzCH$_3$), 5.16 (s, 1H, pzH), 5.79 (s, 1H, pzH), 5.80 (s, 1H, pzH), 5.93 (m, 1H, H−C≡C). ^{13}C{^{1}H} NMR (500 MHz, C_6D_{12}): δ 13.66 (s, pzCH$_3$), 13.80 (s, pzCH$_3$), 13.98 (s, pzCH$_3$), 16.34 (s, pzCH$_3$), 17.51 (s, pzCH$_3$), 17.64 (d, $^1J_{P-C}$ = 32.2 Hz, P(CH$_3$)$_3$), 17.87 (s, pzCH$_3$), 95.15 (m, η^2-HC≡CCF$_3$), 107.44 (s, pzCH), 107.66 (s, pzCH), 108.07 (d, $^4J_{P-C}$ = 4.4 Hz, pzCH), 142.99 (d, $^4J_{P-C}$ = 2.1 Hz, pzCq), 146.07 (s, pzCq), 146.54 (s, pzCq), 152.16 (d, $^3J_{P-C}$ = 4.3 Hz, pzCq), 152.36 (s, pzCq), 153.15 (s, pzCq); the signals for CF$_3$ and η^2- HC≡CCF$_3$ are not detected due to

dx.doi.org/10.1021/ja4080985 | J. Am. Chem. Soc. 2013, 135, 16198−16212

multiple coupling with fluorines. $^{11}B\{^1H\}$ NMR (500 MHz, C_6D_{12}): δ − 8.65 (s). ^{19}F NMR (400 MHz, C_6D_{12}): δ 12.30 (s, 3 F). $^{31}P\{^1H\}$ NMR (C_6D_6): δ 9.64 (d, $^1J_{Rh-P}$ = 135.7 Hz). IR (cm^{-1}): 2133 (C≡C), 2530 (B−H).

*For Tp′Rh(PMe$_3$)(C≡CC$_6$H$_5$)H (**3r**).* The exchange reaction was almost complete after 1 d at ambient temperature. A mixture of **3r** (76%) and Tp′Rh(PMe$_3$)(η^2-CH≡CC$_6$H$_5$) (**3r**-η^2) (24%) was found based on ^1H and $^{31}P\{^1H\}$ NMR spectroscopy. Heating at 140 °C for 1 h in C_6D_6 resulted in the almost quatitative formation of **3r**. Yellow plate crystals (35.8 mg, 82%) of **3r** were grown from 1:1 hexane/ether solution at room temperature. ^1H NMR (500 MHz, THF-d_8): δ −16.53 (dd, $^1J_{Rh-H}$ = 20.6 Hz, $^2J_{P-H}$ = 29.5 Hz, 1H, RhH), 1.58 (d, $^2J_{P-H}$ = 10.4 Hz, 9H, PMe$_3$), 2.23 (s, 3H, pzCH$_3$), 2.30 (s, 3H, pzCH$_3$), 2.39 (s, 3H, pzCH$_3$), 2.42 (s, 3H, pzCH$_3$), 2.46 (s, 3H, pzCH$_3$), 2.64 (s, 3H, pzCH$_3$), 5.56 (s, 1H, pzH), 5.75 (s, 1H, pzH), 5.78 (s, 1H, pzH), 6.95 (t, *J* = 7.4 Hz, 1H, Ph-*p*), 7.08 (t, *J* = 7.7 Hz, 2H, Ph-*m*), 7.17 (d, *J* = 7.1 Hz, 2H, Ph-*o*). $^{13}C\{^1H\}$ NMR (500 MHz, THF-d_8): δ 12.72 (s, pzCH$_3$), 12.94 (s, pzCH$_3$), 12.99 (s, pzCH$_3$), 15.79 (s, pzCH$_3$), 15.96 (s, pzCH$_3$), 17.01 (s, pzCH$_3$), 19.60 (d, $^1J_{PC}$ = 34.8 Hz, P(CH$_3$)$_3$), 103.86 (ddd, $^1J_{Rh-C}$ = 26.53 Hz, $^2J_{P-C}$ = 45.0 Hz, $^2J_{H-C}$ = 3.5 Hz, Rh-C≡C), 105.76 (d, $^4J_{P-C}$ = 3.8 Hz, pzCH), 106.36 (d, $^2J_{Rh-C}$ = 10.8 Hz, Rh−C≡C), 106.98 (s, pzCH), 107.35 (s, pzCH), 124.54 (s, Ph-*ipso*), 128.34 (s, 2C, Ph-*m*), 130.94 (s, Ph-*p*), 131.25 (s, 2C, Ph-*o*), 143.21 (d, $^4J_{P-C}$ = 2.6 Hz, pzCq), 144.49 (s, pzCq), 145.47 (s, pzCq), 150.71 (s, pzCq), 151.00 (d, $^3J_{P-C}$ = 2.3 Hz, pzCq), 152.58 (s, pzCq). $^{31}P\{^1H\}$ NMR (400 MHz, C_6D_6): δ 5.55 (d, $^1J_{Rh-P}$ = 122.8 Hz). IR (cm^{-1}): 2162 (C≡C). Anal. Calcd for $C_{26}H_{37}BN_6PRh\cdot(Et_2O)_{0.5}$: C, 54.65; H, 6.88; N, 13.66. Found: C, 54.71; H, 6.55; N, 13.61.

*For Tp′Rh(PMe$_3$)(η^2-HC≡CC$_6$H$_5$) (**3r**-η^2).* ^1H NMR (400 MHz, C_6D_6): δ 0.68 (d, $^2J_{P-H}$ = 9.7 Hz, 9H, PMe$_3$), 2.17 (s, 3H, pzCH$_3$), 2.38 (s, 3H, pzCH$_3$), 2.41 (s, 3H, pzCH$_3$), 2.47 (s, 3H, pzCH$_3$), 2.63 (s, 3H, pzCH$_3$), 2.72 (s, 3H, pzCH$_3$), 5.07 (s, 1H, pzH), 5.27 (s, 1H, pzH), 5.65 (s, 1H, pzH), 5.85 (d, J_{Rh-H} = 6.3 Hz, 1H, H−C≡C); signals for aryl hydrogens are not detected due to overlap with those of **3r**. $^{31}P\{^1H\}$ NMR (400 MHz, C_6D_6): δ 7.87 (d, $^1J_{Rh-P}$ = 148.6 Hz).

*For Tp′Rh(PMe$_3$)(C≡CC$_6$H$_4$-*p*-CF$_3$)H (**3s**).* The exchange reaction was almost complete after overnight at ambient temperature. A mixture of **3s** (53%) and Tp′Rh(PMe$_3$)(η^2-HC≡CC$_6$H$_4$-*p*-CF$_3$) (**3s**-η^2) (47%) was found based on ^1H and ^{31}P NMR spectroscopy. Heating at 140 °C for 7 h in C_6D_6 resulted in the almost quantitative formation of **3s**. Brown yellow crystals (39.6 mg, 81%) of **3s** were grown from 1:1 hexane/THF solution at room temperature. ^1H NMR (500 MHz, C_6D_6): δ −15.99 (dd, $^1J_{Rh-H}$ = 20.4 Hz, $^2J_{P-H}$ = 29.2 Hz, 1H, RhH), 1.21 (d, $^2J_{P-H}$ = 10.3 Hz, 9H, PMe$_3$), 2.09 (s, 3H, pzCH$_3$), 2.10 (s, 3H, pzCH$_3$), 2.25 (s, 3H, pzCH$_3$), 2.33 (s, 3H, pzCH$_3$), 2.72 (s, 3H, pzCH$_3$), 2.78 (s, 3H, pzCH$_3$), 5.44 (s, 1H, pzH), 5.64 (s, 1H, pzH), 5.78 (s, 1H, pzH), 7.35 (d, *J* = 8.4 Hz, 2H, Ph-*o*), 7.39 (d, *J* = 8.2 Hz, 2H, Ph-*m*). $^{13}C\{^1H\}$ NMR (500 MHz, THF-d_8): δ 12.72 (s, pzCH$_3$), 12.94 (s, pzCH$_3$), 12.99 (s, pzCH$_3$), 15.77 (s, pzCH$_3$), 15.90 (s, pzCH$_3$), 16.03 (s, pzCH$_3$), 19.51 (d, $^1J_{P-C}$ = 34.7 Hz, P(CH$_3$)$_3$), 105.86 (d, $^4J_{P-C}$ = 3.8 Hz, pzCH), 106.09 (d, $^2J_{Rh-C}$ = 10.6 Hz, Rh−C≡C), 107.11 (s, pzCH), 107.45 (s, pzCH), 111.9 (dd, $^1J_{Rh-C}$ = 26.5 Hz, $^2J_{P-C}$ = 45.7 Hz, Rh-C≡C), 125.43 (q, $^3J_{F-C}$ = 3.7 Hz, 2C, *p*-CF$_3$−C$_6$H$_4$-*m*), 125.86 (q, $^1J_{F-C}$ = 270.5 Hz, CF$_3$), 131.48 (s, 2C, *p*-CF$_3$−C$_6$H$_4$-*o*), 132.73 (q, $^2J_{F-C}$ = 18.0 Hz, CCF$_3$), 134.67 (s, *p*-CF$_3$−C$_6$H$_4$-*ipso*), 143.42 (d, $^4J_{P-C}$ = 2.8 Hz, pzCq), 144.67 (s, pzCq), 145.67 (s, pzCq), 150.84 (s, pzCq), 150.93 (d, $^3J_{P-C}$ = 2.6 Hz, pzCq), 152.53 (s, pzCq). $^{31}P\{^1H\}$ NMR (400 MHz, C_6D_6): δ 5.37 (d, $^1J_{Rh-P}$ = 122.2 Hz). ^{19}F NMR (400 MHz, C_6D_{12}): δ 1.39 (s). IR (cm^{-1}): 2110 (C≡C). Anal. Calcd for $C_{27}H_{36}BF_3N_6PRh\cdot THF_{0.45}$: C, 50.96; H, 5.88; N, 12.38. Found: C, 50.95; H, 5.48; N, 12.28.

*For Tp′Rh(PMe$_3$)(η^2-CH≡CC$_6$H$_4$-*p*-CF$_3$) (**3s**-η^2).* ^1H NMR (400 MHz, C_6D_6): δ 0.61 (d, $^2J_{P-H}$ = 9.8 Hz, 9H, PMe$_3$), 2.00 (s, 3H, pzCH$_3$), 2.09 (s, 3H, pzCH$_3$), 2.34 (s, 3H, pzCH$_3$), 2.36 (s, 3H, pzCH$_3$), 2.39 (s, 3H, pzCH$_3$), 2.59 (s, 3H, pzCH$_3$), 5.27 (s, 1H, pzH), 5.33 (br, 1H, H−C≡C), 5.88 (s, 1H, pzH), 5.95 (s, 1H, pzH), 7.39 (d, *J* = 6.0 Hz, 2H, Ph-*o*), 7.63 (d, *J* = 7.9 Hz, 2H, Ph-*m*). ^{19}F NMR (400 MHz, C_6D_{12}): δ 1.48 (s). $^{31}P\{^1H\}$ NMR (400 MHz, C_6D_6): δ 8.02 (d, $^1J_{Rh-P}$ = 146.0 Hz).

■ ASSOCIATED CONTENT

Ⓢ Supporting Information

Kinetic treatments for reductive elimination reactions and competition experiments, NMR spectra, DFT calculations, and details of X-ray analysis. This material is available free of charge via the Internet at http://pubs.acs.org. CCDC 953348−953363.

■ AUTHOR INFORMATION

Corresponding Author

jones@chem.rochester.edu

Notes

The authors declare no competing financial interest.

■ ACKNOWLEDGMENTS

Acknowledgment is made to the U.S. Department of Energy (Grant No. FG02-86ER-13569) for their support of this work.

■ REFERENCES

(1) Gol'dshleger, N. F.; Es'kova, V. V.; Shilov, A. E.; Shteinman, A. A. *Zh. Fiz. Khim.* **1972**, *46*, 1353.
(2) Anastas, P. T.; Warner, J. C. *Green Chemistry: Theory and Practice*; Oxford University Press: New York, 1998, p 30.
(3) Fisher, B. J.; Eisenberg, R. *Organometallics* **1983**, *2*, 764.
(4) Kunin, A. J.; Eisenberg, R. *J. Am. Chem. Soc.* **1986**, *108*, 535.
(5) Kunin, A. J.; Eisenberg, R. *Organometallics* **1988**, *7*, 2124.
(6) Jones, W. D.; Feher, F. J. *Organometallics* **1983**, *2*, 686.
(7) Jones, W. D.; Kosar, W. P. *J. Am. Chem. Soc.* **1986**, *108*, 5640.
(8) Jones, W. D.; Foster, G. P.; Putinas, J. *J. Am. Chem. Soc.* **1987**, *109*, 5047.
(9) Jones, W. D.; Hessell, E. T. *Organometallics* **1990**, *9*, 718.
(10) Jones, W. D.; Hessell, E. T. *J. Am. Chem. Soc.* **1992**, *114*, 6087.
(11) Hsu, G. C.; Kosar, W. P.; Jones, W. D. *Organometallics* **1994**, *13*, 385.
(12) Wick, D. D.; Reynolds, K. A.; Jones, W. D. *J. Am. Chem. Soc.* **1999**, *121*, 3974.
(13) Hong, P.; Yamazaki, H.; Sonogashira, K.; Hagihara, N. *Chem. Lett.* **1978**, 535.
(14) Murai, S.; Kakiuchi, F.; Sekine, S.; Tanaka, Y.; Kamatani, A.; Sonoda, M.; Chatani, N. *Nature* **1993**, *366*, 529.
(15) Kakiuchi, F.; Yamamoto, Y.; Chatani, N.; Murai, S. *Chem. Lett.* **1995**, 681.
(16) Crabtree, R. H.; Mihelcic, J. M.; Quirk, J. M. *J. Am. Chem. Soc.* **1979**, *101*, 7738.
(17) Crabtree, R. H.; Quirk, J. M. *J. Organomet. Chem.* **1980**, *199*, 99.
(18) Crabtree, R. H.; Mellea, M. F.; Mihelcic, J. M.; Quirk, J. M. *J. Am. Chem. Soc.* **1982**, *104*, 107.
(19) Goldberg, K. I., Goldman, A. S., Eds. Organometallic C-H Bond Activation: An Introduction. *Activation and Functionalization of C−H Bonds*; ACS Symposium Series 885; American Chemical Society: Washington, DC, 2004; Chapter 1.
(20) Chen, H.; Hartwig, J. F. *Angew. Chem., Int. Ed.* **1999**, *38*, 3391.
(21) Iverson, C. N.; Smith, M. R., III *J. Am. Chem. Soc.* **1999**, *121*, 7696.
(22) Chen, H.; Schlecht, S.; Semple, T. C.; Hartwig, J. F. *Science* **2000**, *287*, 1995.
(23) Hall, J. C.; Perutz, R. N. *Chem. Rev.* **1996**, *96*, 3125.
(24) Buchanan, J. M.; Stryker, J. M.; Bergman, R. G. *J. Am. Chem. Soc.* **1986**, *108*, 1537.
(25) Bryndza, H. E.; Fong, L. K.; Paciello, R. A.; Tam, W.; E., B. J. *J. Am. Chem. Soc.* **1987**, *109*, 1444.
(26) Bennett, J. L.; Wolczanski, P. T. *J. Am. Chem. Soc.* **1994**, *116*, 2179.
(27) Bennett, J. L.; Wolczanski, P. T. *J. Am. Chem. Soc.* **1997**, *119*, 10696.
(28) Schaller, C. P.; Wolczanski, P. T. *Inorg. Chem.* **1993**, *32*, 131.

(29) Bulls, A. R.; Bercaw, J. E.; Manriquez, J. M.; Thompson, M. E. *Polyhedron* **1988**, *7*, 1409.
(30) We later discovered that this is not strictly a correct assumption, because a statistical correction for the number of hydrogens that can be activated contributes to the entropy of the equilibrium; for example, for benzene versus methane there is a 6:4 statistical preference for benzene, which contributes to the free energy for the equilibrium (= RT ln(#H_1/#H_2)). Calculations in refs 31, and 33−37 include this correction, whereas refs 24−29 and 32 did not.
(31) Jones, W. D.; Hessell, E. T. *J. Am. Chem. Soc.* **1993**, *115*, 554.
(32) Wick, D. D.; Jones, W. D. *Organometallics* **1999**, *18*, 495.
(33) Choi, G.; Morris, J.; Brennessel, W. W.; Jones, W. D. *J. Am. Chem. Soc.* **2012**, *134*, 9276.
(34) Evans, M. E.; Li, T.; Vetter, A. J.; Rieth, R. D.; Jones, W. D. *J. Org. Chem.* **2009**, *74*, 6907.
(35) Jiao, Y.; Evans, M. E.; Morris, J.; Brennessel, W. W.; Jones, W. D. *J. Am. Chem. Soc.* **2013**, *135*, 6994.
(36) Evans, M. E.; Burke, C. L.; Yaibuathes, S.; Clot, E.; Eisenstein, O.; Jones, W. D. *J. Am. Chem. Soc.* **2009**, *131*, 13464.
(37) Tanabe, T.; Brennessel, W. W.; Clot, E.; Jones, W. D. *Dalton Trans.* **2010**, *39*, 10495.
(38) Clot, E.; Mégret, C.; Eisenstein, O.; Perutz, R. N. *J. Am. Chem. Soc.* **2009**, *131*, 7817.
(39) Low efficiency of irradiation may be due to the presence of a maximum UV−vis absorbance for **1** at 226 nm (ε = 13237 cm^{-1} M^{-1}) (see Supporting Information) while the photolysis was conducted with a 270−370 nm band-pass filter. Moreover, the irradiation excites not only **1** but also the newly born Tp′Rh(PMe_3)(R)H, which can undergo bimolecular redistribution to form dialkyl and bisphosphine complexes.[37] The formation of (κ^2-Tp′)Rh(PMe_3)$_2$ has also been observed in the reductive elimination of Tp′Rh(PMe_3)(Ar^F)H in C_6D_6 at above 120 °C.
(40) Northcutt, T. O.; Wick, D. D.; Vetter, A. J.; Jones, W. D. *J. Am. Chem. Soc.* **2001**, *123*, 7257.
(41) Wick, D. D.; Jones, W. D. *Inorg. Chim. Acta* **2009**, *362*, 4416. Paneque, M.; Perez, P. J.; Pizzano, A.; Poveda, M. L.; Taboada, S.; Trujillo, M.; Carmona, E. *Organometallics* **1999**, *18*, 4304.
(42) Vetter, A. J.; Flaschenriem, C.; Jones, W. D. *J. Am. Chem. Soc.* **2005**, *127*, 12315.
(43) Northcutt, T. O.; Lachicotte, R. J.; Jones, W. D. *Organometallics* **1998**, *17*, 5148.
(44) Luo, Y. *Comprehensive Handbook of Chemical Bond Energies*; CRC Press: Boca Raton, FL, 2007.
(45) A reviewer suggested that perhaps the difference in slopes can be accommodated by there being an agostic interaction of the neopentylisocyanide ligand with the vacant site on the 16-electron Rh(I) intermediate. Examination of the X-ray structures of these molecules, however, reveals that the linearity of the Rh−C−N−C linkage places the methyl hydrogens too far from the metal to form σ-complexes.
(46) Uddin, J.; Morales, C. M.; Maynard, J. H.; Landis, C. R. *Organometallics* **2006**, *25*, 5566.
(47) Wick, D. D.; Jones, W. D. *Inorg. Chem.* **1997**, *36*, 2723.